I
Methodologies and Instrumentation

Advances in Flow Analysis. Edited by Marek Trojanowicz

ISBN: 978-3-527-31830-8

1
Theoretical Aspects of Flow Analysis

Fernando A. Iñón and Mabel B. Tudino

1.1
Introduction

Flow injection analysis (FIA) arises as a consequence of the growing trend towards automation in chemical analysis, and as a natural evolution of the so-called "continuous flow analysis" (CFA) which has revolutionized the conception of chemical analysis, especially in the field of clinical analysis and sample manipulation.

FIA belongs to a family of analytical methods based on the injection of a sample (containing the analyte or its reaction products) into a non-segmented carrier stream, which in turn carries it through a chemical or physical modulator towards the detector. To this category of methods belong also the different chromatographies and capillary electrophoresis. Figure 1.1a depicts the block diagram common to all these methods. Methods are thus differentiated by the nature of the "modulator" which transforms the square wave (the injection) into a chromatogram, electroferogram, or just a FIA peak (fiagram) (Figure 1.1b).

Thus, the differences between these techniques may be better understood in terms of the modulator function and the prevailing forces (or properties) interacting with it.

The primary difference between FIA and chromatography lies in the mass transfer between two phases that exists in the latter, but the diversity of FIA systems published to date makes it difficult to draw a dividing line between the two techniques.

The main difference between chromatography and FIA lies in the fact that in the former separations are achieved through a repetition of interactions which modulate the differential migration rate of the species through the system, while FIA exploits chemical reactions that transform the analytes into species which may be quantified by a detector.

Advances in Flow Analysis. Edited by Marek Trojanowicz

ISBN: 978-3-527-31830-8

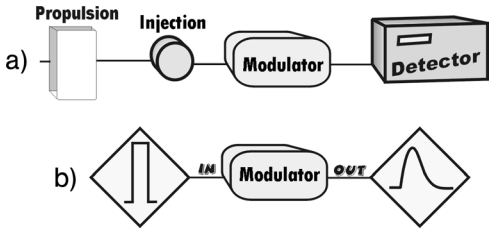

Figure 1.1 Stimulus-response in flow systems.

1.2
Classification of Flow Systems. Fundamentals

1.2.1
Continuous Flow Analysis

CFA, introduced by Skeggs [1], relies on the fact that the sample and the reactive react while traveling in the tube that conducts them to the detector. Air bubbles separate the portions of fluid (reactive) in order to diminish the longitudinal dispersion of the sample and the interaction between samples (carry over), which in turn favor mixing and increase the analysis frequency.

1.2.2
Flow Injection Analysis

In 1975 Růžička and Hansen introduced FIA [2] (calling it initially *non-segmented continuous flow analysis*) showing that bubble separation was unnecessary to prevent carry over and that it also introduced uncertainty in the reproducibility of the sample residence time inside the system. With the non-segmented technique the integrity of the sample pulse is kept by careful control of the hydrodynamic conditions of the system. The analytical consequence is important: in CFA the detection should be performed once the reaction is finished (once equilibrium has been reached) while in FIA this condition is unnecessary. Although in CFA equilibrium is usually attained, and thus the sensitivity is the same as for "batch" techniques, it is not possible to exploit chemical kinetics and mixing kinetics (gradient techniques) as variables to adjust the analytical response. This fact should be added to the difficulty posed by the presence of air bubbles in certain detection systems.

1.2.3
Sequential Injection Analysis

Sinusoidal flow systems [3] avoid fast delivery of the sample to the detector (shortening also the distance to be covered by the sample) in order to allow better mixing and more complete reaction between the sample and the reagents. This is accomplished by a fast change in the carrier flow direction (back and forward) until the desired degree of reaction is reached. This technique results in a drastic reduction

in consumption of reagents but at the same time reduces the analytical frequency to a half (typically). Sequential injection analysis (SIA) is based on this principle [4–6].

SIA appeared as a response to two essential problems found in FIA: the increased complexity of the manifolds employed, and the need for its use in process control. The former is a consequence of the addition of steps to a given system, giving rise to many working channels, which in turn leads to higher reagent consumption and very difficult "tuning" of the system. The latter, requires systems that are robust, reliable and stable in the long term and which could proceed unmanned and with low reagent consumption.

FIA, being a continuous flow system, presents several disadvantages such as high consumption of samples and reagents, a need for constant supervision of the peristaltic pumps, frequent recalibration and manual adjustment of the system. These facts are not a problem on the laboratory scale, but become a major issue when dealing with industrial process control.

SIA tackles these difficulties by simplifying the system: a single piston pump (which allows precise flow control in both directions), a single flow channel and only one selecting (instead of injection) valve, are used. Through this valve accurately measured volumes of carrier, sample and reagents are introduced into the reaction coil. Once this step is accomplished, the valve is changed to direct the flow towards the detector. During this step mixing is accomplished through back and forth movements, and finally in one direction to transport the reaction coil load to the detector.

On the other hand, the complexity of multiple channel FIA systems is reduced in SIA systems by using mostly single lines around a selecting valve. Operational parameters in SIA are: volume taken of each solution, flow rate, and the time in which the flow is stopped or changes its direction. Occasionally more pumps could be needed (one for each line) which makes controlling the system very difficult. On-line dilution is still an issue in SIA systems as the sample pulse is greatly dispersed and hence its signal profile becomes much distorted [7–9].

1.2.4
Multicommutation in Flow Injection Analysis

Multi-commuting arose as a FIA modification directed towards increasing the versatility of flow systems, diminishing reagent consumption, improving mixing and facilitating automation. This concept was first mentioned in the 1980s [10, 11], but was only formally introduced in 1994 [12] since when numerous papers have shown its potential [13, 14]. One of the main advantages of this technique lies in exploiting successive injections of sample and carrier (tandem stream [12]) in which the volumes of each section are easily selected.

In this technique three-way solenoid valves are employed and controlled temporally through a microprocessor. System designs are usually simple and it is easy to imagine that, depending on the set-up, the advantages of the technique may be fully exploited and compared with FIA or SIA systems. (See Figure 1.2.)

Multi-commuting appears to be the technique which has the advantages of FIA together with those of SIA and overcomes all their disadvantages [13].

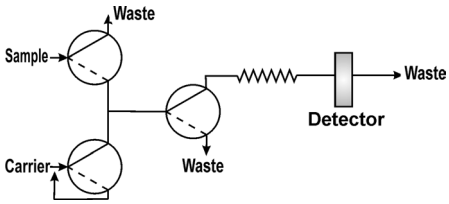

Figure 1.2 Multicommuted system.

Definitely, the key to optimizing a flow technique lies in balancing the dispersion of the injected pulse and reagent mixing, taking into account the time required to reach the optimal degree of conversion of reagents into detectable species.

1.2.5
Stopped Flow

Amongst modern techniques derived from FIA, it seems that "*stopped flow*" techniques are the easiest to implement and the most versatile [15]. In these techniques, the sample is injected as in conventional FIA but the carrier flow is stopped when the sample and the reagents reach the flow cell (at the detector) giving rise to several advantages [15, 16]. While physical dispersion is minimized, as the driving force is diffusion only, chemical reaction proceeds (uncoupling both processes) increasing sensitivity as there is a longer reaction time and lower dispersion of the products. Thus, reagent consumption and waste production diminish and, by controlling the stopping time, the concentration range can be selected, which is of the utmost importance for kinetic determinations at different wavelengths. However, stopped flow has the disadvantage of requiring a very robust and reproducible time control in order not to affect precision.

1.2.6
Batch Flow Injection Analysis (BFA)

Batch flow injection analysis was proposed by Honorato *et al.* [17] as an alternative way to carry out titrations in flow systems. Sampling and signal processing are done as in usual flow systems, whereas chemical reactions take place in a reaction chamber similar to those found in batch systems. The approach is then a flow–batch hybrid system combining the intrinsic advantages of flow systems, such as high sampling rate, low sample and reagent consumption, low cost, ease of automation, and so on, with the wide application range inherent to batch systems.

The method is based upon the use of three three-way solenoid valves to transmit the fluids inside the reaction chamber and to the reactor where a magnetic stirrer ensures instantaneous homogenization of the cell. Reproducible selection of the added aliquots is found for ON/OFF valve intervals controlled by a personal computer.

1.3
Dispersion in Flow Injection Analysis: From the Movement of Fluids in Open Tubes to Controlled Dispersion

A fluid is any kind of substance that can support a shear force when it is not in motion and undergoes a continuous change when it is stressed. A fluid is ideal when, in motion, it cannot transfer or transport heat from one portion to another, nor produce friction with the inner surface of the tube. This can also be defined as an ideal fluid has no viscosity. Obviously, all fluids used in analytical chemistry have viscosity, that is, inner friction. If viscosity is independent of time for any applied shear force, the fluid is known as Newtonian (such as water). The viscosity of non-Newtonian fluids depends on shear force modulus and time (even for a constant shear force). Most carriers used in flow systems are aqueous solutions that can be considered Newtonian, therefore only Newtonian fluids are normally considered.

Fluidynamics is the science devoted to the study of fluids and has a plethora of applications in other fields: biology, chemistry, engineering, medicine, and so on. It is based on the conservative laws (such as mass, movement, energy and thermodynamics) and constituent laws (i.e., Fick's first law that establishes the dependence of mass transfer on concentration gradients). With this set of laws a series of differential equations can be written for any process, from which it may be possible to infer, predict or describe the whole process.

Nevertheless, mathematical solutions to these equations are rarely found for real systems. On the other hand, many constituent laws are empirical [18], and their coefficients (viscosity, diffusion, etc.) are only known under certain experimental conditions and in many cases cannot be extrapolated to real systems.

Transport phenomena is the area of fluidynamics devoted to the study of different types of transport under different experimental conditions (i.e., dimensions of the system, geometry, etc., type of fluids, etc.). One of their objectives is to provide equations applied to reduce systems, that is, systems whose actual size is normalized by some parameter which requires the definition of adimensional numbers (i.e., Reynolds, Schmidt, Peclet numbers, etc.). The transport process in a real-size system can be explained by considering the transport process in its reduced dimension.

1.3.1
Transport of Fluids

It is worth stressing the difference between the transport process and transport phenomena: the process is the phenomena integrated in a given dimension (spatial or temporal). Transport laws are based on the two most relevant properties of fluids: viscosity and thermal conductivity and, in the case of solutions, diffusivity. Transport properties, in contrast to equilibrium, are related to the velocity of a given process.

1.3.1.1 Viscosity

Viscosity (η) is the capacity of a fluid to resist deformation and depends on the composition of the fluid and its temperature. For Newtonian fluids, η is the

proportional coefficient between the tangential shear force and the generated velocity gradient normal to this force.

For aqueous solutions, viscosity can be calculated using Equation (1) [19].

$$\ln\left(\frac{\eta(20\,^{\circ}\mathrm{C})}{\eta(T)}\right) = \frac{1.37023\cdot(T-20)+8.36\cdot10^{-4}(T-20)^2}{109+T} \tag{1}$$

where $\eta(20\,^{\circ}\mathrm{C}) = 1$ cp (centi-poise, 1×10^{-3} Pa s). Diffusion coefficients, or at least their order of magnitude, can be predicted knowing η.

Kinematic viscosity is the ratio between the viscosity and the density (δ) of a fluid, and its units are square length divided by time ($1\times10^{-6}\,\mathrm{m^2\,s^{-1}}$ for water at 20 °C). Kinematic viscosity is useful when comparing mass transfer ratios by normalizing diffusion coefficients.

From the analytical point of view, the viscosity of different samples must be kept as constant as possible because the concentration gradient profile inside a flow system, and thus its instrumental response, depends drastically on this property, as was studied by Brooks *et al*. [20].

Moreover, when there is a sharp difference between sample and carrier solutions, there is a spurious signal in most detectors, known as Schlieren effect, that drastically affects detection limits. In order to minimize this error source, Betteridge and Růžička [21] suggest that the viscosity of standard and sample solutions must be identical. Another possibility is to include a mixing chamber [22] with a magnetic stirrer when it is not possible to match viscosity. This strategy is mainly used in BFA.

1.3.1.2 **Thermal Conductivity**

This is the capacity of the fluid to transport heat by conduction and depends on the fluid composition and its temperature. Some methods require heating of some parts of the flow system and this property allows one to dimension the heat.

1.3.1.3 **Diffusivity**

As viscosity refers to moment transfer and heat conductivity to heat transfer, diffusivity refers to mass transfer. It is related to the velocity of molecules that travel in a "sea" of other molecules (actually, the 'sea' can also be the same substance and in this case the term is called autodiffusivity). It depends on temperature, molecule/particle size and the strength of intermolecular forces. Diffusivity in the solid state is extremely low, and in liquids it is lower than in gases. Differently from the diffusivity in the gas phase, where the diffusivity of gas A in gas B is nearly equal to the diffusivity of gas B in gas A, the diffusivity of solute A in solvent B almost always is very different to the diffusivity of solute B in solvent A.

1.3.1.4 **Diffusion**

Diffusion is a transport phenomenon that refers to the movement of solutes in the absence of any convective contribution and it is a consequence of a difference in chemical potential, due to a difference in the activity of the solute, in a given direction of the fluid. Any difference in activity (concentration in dilute solutions) tends to be homogenized by the diffusion process, even in the absence of advection.

The net flux of mass in a given direction depends on the concentration gradient in the same direction. This diffusive flux can be represented as a vector with components J_x, J_y, J_z defined in Equation (2):

$$J_x = -k\frac{\partial C}{\partial x} \quad J_y = -k\frac{\partial C}{\partial y} \quad J_x = -k\frac{\partial C}{\partial z} \tag{2}$$

where C is the concentration of the solute, and x, y, and z the axis directions. These equations are known as Fick's first law and k is known as the diffusion coefficient (D_m) of that solute in this medium. This law means that the Brownian movement causes, on average, a net flux of solute from a more concentrated to a less concentrated region of the fluid.

The magnitude of the diffusion coefficient in gases is around 10^{-5} to $10^{-4}\,m^2\,s^{-1}$ (at atmospheric pressure), whereas in liquids it is typically around 10^{-10} to $10^{-9}\,m^2\,s^{-1}$. Diffusion coefficients increase with temperature and their magnitude depends on changes in molar density, pressure and viscosity. Diffusion in flow systems plays a very important role and has enormous analytical implications, as will be discussed in this chapter. Nevertheless, for working with flow injection systems, the convective mass transport needs to be taken into account.

1.3.2
The Diffusion–Convection Equation in Open Conduits

Mass transport inside a fluid travelling inside a pipe can be iso, endo or exothermic. Non-isothermic changes will produce changes in fluid properties such as viscosity [18, 23]. For Newtonian, uncompressible (constant density), constant viscosity (isothermic change) fluids flowing inside a cylindrical pipe it is possible to derive Equation (3). It considers convective transport based on a linear velocity (u) independent of the z coordinate, but dependent on the radial coordinate (Figure 1.3). This is only strictly true in perfectly straight open tubes with constant inner diameter, without any curvature, perturbations and splices as they will alter velocity profile.

$$\frac{\partial C}{\partial t} + u(r)\cdot\frac{\partial C}{\partial z} = D_m\cdot\left(\frac{1}{r}\frac{\partial C}{\partial r} + \frac{\partial^2 C}{\partial r^2} + \frac{\partial^2 C}{\partial^2 z}\right) \tag{3}$$

The concentration as function of time depends on convection, represented by the second left-hand term, and the diffusive transport, represented by the right-hand side of the equation. It can be clearly noted that diffusion influences both radial and axial mass transport.

Convection, coaxial to the flow movement, together with diffusion are the main causes of axial dispersion in tubes. Taylor [24, 25] and Levenspiel [26] are pioneers

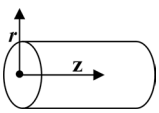

Figure 1.3 Coordinates definition.

in the theoretical study of transport and dispersion inside tubes and their works set the basis for theoretical studies and modeling of dispersion in the field of flow analysis systems.

Particularly for FIA, Růžička and Hansen [27] have provided the first theoretical aspects for describing processes inside these systems. It must be taken into account that the differential Equation (3) has no general solution and its applicability in any system is based on several assumptions.

1.3.3 The Distribution of Times of Residence

The residence time of the substance, related to the residence time of each fluid element, inside a system is one of the key factors in FI and it depends on the design and operational parameters of the system (size, flow rate, geometry, etc.). This task requires knowledge of the residence time distribution (RTD) of the different portions of injected substance inside the system plus all balances related to mass, composition of chemical reactants and heat transfers.

Experimentally, RTD curves are obtained by introducing a tracer (i.e., a colored substance) and recording the concentration of that tracer in the outlet of the system (i.e.,by measuring the absorbance at the characteristic absorption wavelength of the substance), see Levenspiel [26]. RTD curves can be normalized using Equation (4): the area under the curve is equal to 1, supposing that all tracer elements leave the system.

$$\int_{t=0}^{\infty} E(t)\partial t = 1 \tag{4}$$

$$t_m = \int_{t=0}^{\infty} t \cdot E(t)\partial t \tag{5}$$

where E is the fraction of fluid with an age t. $E(t)$ is characteristic of a given flow pattern. Knowledge of the RTD profile may help one to know the flow profile inside the system and to develop a quantitative expression to describe system dispersion. The mean time of residence (t_m) can be calculated using Equation (5).

A common variable reduction for comparing different systems is by using the ratio of the time (t) and the mean time of residence (t_m). This ratio is expressed by the adimensional number θ equal to $t \cdot t_m^{-1}$.

There are different ways in which RTD curves can be displayed. "*C-curves*," are the equivalent to the E curve displayed in Figure 1.4 and are calculated by dividing the concentration of the tracer at the output of the system ($C(t)$) by the area under the curve. "*F-curves*" are those obtained when $C(t) \cdot C_0^{-1}$ is calculated as a function of time, and can be associated to the integral of the C-curve. Figure 1.5 shows these curves for systems under three different flow regimes: plug-flow, ideally mixed and arbitrary flow. The dispersion of a given system is inversely related to the slope of its F-curve and directly related to the width of its C-curve.

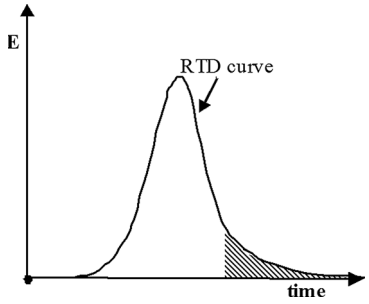

Figure 1.4 Residence times curve.

Taylor [24] has shown that with dimensions similar to an analytical flow system, diffusion has a key role. Although axial diffusion may be negligible compared to convection, radial diffusion is always important and, for small i.d. tubes and low flow rates, it may represent the principal component of dispersion.

1.3.3.1 Characterization and Experimental Domain of Flow Systems: Dimensionless Numbers and Their Meaning

Many adimensional numbers have been defined in order to characterize hydraulics in flow systems, based upon linear flow rate (u), diffusion coefficient (D_m), time (t), reactor length (L), tube radii (a), and so on. The main objective of these adimensional variables is the integration of differential equations, such as Equation (3), for a group of similar systems and not for each particular one. Painton and Mottola [28, 29] have been pioneers of the use of adimensional numbers in FIA.

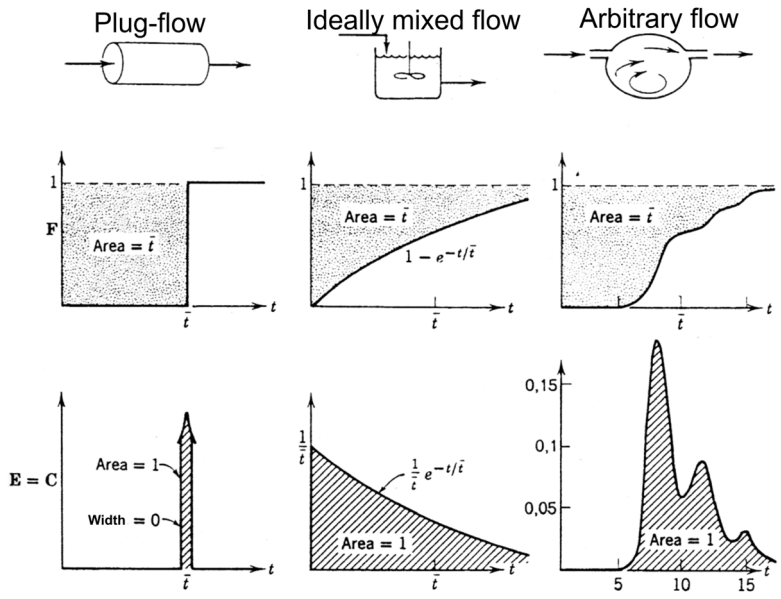

Figure 1.5 E, C, and F curves for different flow profiles.

Table 1.1 Definition of adimensional numbers.

Reynolds (Re)	Peclet (Pe_L)	Peclet radial (Pe_r)	Fourier (τ)	Schmidt (Sc)
$2 \cdot \bar{u} \cdot a \cdot \left(\frac{\eta}{\delta}\right)^{-1}$	$\frac{\bar{u} \cdot L}{D_m}$	$\frac{\bar{u} \cdot a}{D_m}$	$\frac{D_m \cdot t_m}{a^2}$	$\frac{\eta}{\delta} \cdot \frac{1}{D_m}$

The most common reduced numbers used in analytical flow systems are: Peclet, Schmidt, Fourier and Reynolds, and are defined as shown in Table 1.1.

The Reynolds number is a balance between inertial forces ($\delta \cdot \bar{u}^2/a$, transport moment by convection) and viscous forces ($\eta \cdot \bar{u}/a^2$, transport moment by diffusion) and indicates the flow regimen inside a tube. For straight tubes, Re lower than 2000 indicates laminar flow, which means that the flow lines of the fluid elements are parallel to the direction of the flow. There is not a given Re number from which the flow pattern becomes turbulent and there is a transition zone typified by a mixed flow regime. The end of the transition zone is characterized by a critical Reynolds number (Re_c) that, for straight tubes, is around 2300. Coiled tubes stabilize laminar flow, incrementing Re_c as the ratio between the tube i.d. and coil diameter increases.

Radial Peclet, or reduced rate [30], relates mass transport by convection ($\bar{u} \cdot \Delta C/a$) to mass transport by diffusion ($D \cdot \Delta C/a^2$). The axial Peclet number (Pe_L) compares axial mass transport by convection to that of diffusion. A similar, but not the same, ratio is more commonly used in analytical flow systems and is known as the reduced distance $\left(\frac{D_m \cdot L}{2\bar{u} \cdot a^2}\right)$. Gunn and Pryce (see [31]), have shown that for relatively small Re numbers (0.02–420) there is a dependence between radial and axial Pe numbers with Re number.

The inverse of Pe_L has been defined in the chemical engineering field as "*reactor dispersion number*" (D_N) and has been used to describe RTD variance, which is a dispersion estimator (see next section) [26]. At higher Pe_L convection dominates transport, whereas small values indicate greater influence of diffusion.

The Fourier number (τ) does a scale reduction similar to the Peclet number but in time coordinates, comparing residence time with molecular diffusion. High τ values indicate a higher diffusion contribution to mass transport, whereas small values are related to a higher contribution from convection.

The Schmidt number relates solute and fluid properties instead of flow characteristics. High Sc values (moment diffusion higher than molecular diffusion) are common in liquids (Sc values ranging between 100 and 10 000 are found in aqueous solutions) and shows that convection prevails over diffusion. Pe can be calculated as the product between Re and Sc.

1.3.4 From the RTD Curve to the Generation of Signals in Flow Injection Systems

1.3.4.1 The Dispersion Process

Taylor [24, 25] has published the first experimental and theoretical contributions devoted to understanding the dispersive process inside small i.d. tubes. He studied

different stages related to the introduction of a chemically-inert solute into the fully developed laminar flow pattern of a solvent flowing inside a cylindrical pipe.

It was observed [24] that for short times (high linear velocity), axial convection is the main transport and thus the main contribution to the increase in dispersion of the solute zone. For longer times, radial molecular diffusion contributes to the dispersion process. The net effect of molecular diffusion is to reduce axial stretching of the solute zone, thus decreasing axial dispersion. For even longer times, molecular diffusion continues to limit axial dispersion, generating a more uniform concentration of the solute zone. At longer times, axial and radial diffusion contributes to dispersion, and the solute zone can be regarded as a plug in which the concentration profile in the axial directions tends to be Gaussian. It is important to notice that this does not mean the absence of a radial velocity profile. These conditions are never reached in FIA or multicommutation systems.

Analytical resolution of the convective-diffusion equation (Equation (3)) is only available under two extreme boundary conditions: (i) mass transport is only due to convective transport (short residence times) and (ii) diffusive transport is the main transport phenomenon contributing to dispersion (long residence times). Under these boundary conditions, analytical flow systems are not well represented.

1.3.4.2 **The Concept of Controlled Dispersion and Analytical Implications**

A consequence of dispersion is the loss in sensitivity and limit of detection. So, from the analytical point of view, the dispersion is a determinant factor in the performance of the system of analysis. In flow systems the term dispersion was associated directly with the loss of sensitivity in comparison with that obtained when the stationary state is reached. Even though this is a consequence, it does not describe the dispersion phenomenon which involves physical and chemical dispersion.

Physical dispersion is the result of the processes of spatial redistribution of mass that undergoes the pulse injected into a carrier in the absence of chemical reaction. This redistribution is carried out due to the parabolic linear velocity profile in non-segmented flow systems. A consequence of this profile is the appearance of a radial concentration gradient that tends to be homogenized by diffusion and, when they exist, by the presence of secondary flows (in directions other than that of the principal flow).

When a chemical reaction is involved, the term chemical dispersion is considered and it is related to the degree of completion of the reaction at the moment of detection (general case in FIA). Thus, chemical dispersion is always accompanied by physical dispersion, since it depends on both the mixing of reagents and the redistribution of the formed product. The concentration gradient affects the kinetics of the reaction and this in turn modifies the gradient [28]. It should be understood that, from the theoretical point of view as opposed to the experimental one, the study of the chemical dispersion is highly complex and needs numerous simplifications to approach it.

"Dilution" is a term that many authors [16, 20, 32–34] erroneously associate with the term "dispersion." However, dilution can be understood as a particular case of dispersion where the function of redistribution of mass is homogeneous in time and space, which is not the situation in FI where the term dispersion is more suitable. So,

in FIA it is only possible to talk of an average dilution of the sample in a transverse section of fluid, but this average dilution is not indicative of the way in which the dispersive process was carried out.

The process of dispersion has its origin in the inhomogeneity that is imposed on a substance when it is submitted to diverse types of gradients. In flow systems, the injection of a pulse of substance in a carrier that flows submits the substance to two types of gradient: one of mass and one of velocities (or in general of moments). The diverse ways in which the dispersion takes place is a result of the homogenization of these gradients. These complex processes involve the study of redistribution of mass and energy from their original distribution to that obtained in the outlet of the systems. However, as the dispersion process can be controlled, trustworthy analytical results can be obtained.

1.3.4.3 **The Transient Profile**

When a sample/tracer is injected into a flow system, its spatial distribution changes and this change depends upon different dimensional and operational variables of each part of the flow system. The signal profile obtained by locating a detector at the system outlet is directly related to the spatial and temporal distribution of the sample plug. Taylor [24, 25] and Levenspiel [35, 36] have studied these cause/effect relationships.

From the analytical point of view, the information required to relate the concentration domain to the domain of a measurable variable (i.e., voltage) is obtained through the response signal. In flow systems, this response can be of two kinds: (i) the steady state signals obtained when sample, reactants and carrier are homogenized and all possible reactions reach their equilibrium and (ii) dynamic signals obtained when a limited portion of the sample undergoes a dispersion process in a given carrier and the possible chemical reaction may or not reach equilibrium.

In the last case, the concentration profile must only depend on analyte concentration and the reproducibility of this profile is essential.

In CFA systems, it is important to reach a *plateau*. Under this condition it is possible to improve precision by averaging the response signal n at the top of the plateau. Moreover, as equilibrium is reached, the sensitivity is usually higher than in other flow systems, but the sample throughput is decreased and sample and reactants consumption increases [37].

The asymmetric peak observed in FIA systems is due to the influence of the injection mode and the contribution of convection and diffusion to mass transport.

A common approach is to try to fit a response signal by a given model and, in the case of peaks, the Gaussian model is one of the simplest to apply. In FIA systems, signals obtained under high dispersion conditions can be fitted by a Gaussian model. If dispersion is medium to high, it can be described as an exponential modified Gaussian (EMG) [38]. When dispersion is low or medium to low, there is no general model to fit a FIA peak.

The interdispersion of sample plug and carrier solution is mandatory in FIA. It is expected that if the analytical response is due to the concentration of a given analyte in the sample, its maximum will be located at the maximum concentration of the analyte in the sample plug. Nevertheless, if a product of the reaction between the analyte and

the carrier is monitored this assumption is usually false as it depends on the ratio analyte:reactant which optimizes the chemical reaction.

The operational and design parameters that have the greatest influence on the carrier/sample interdispersion are: tube radius, spatial and geometrical disposition of the reactor/manifold, flow rate, injection and reactor volume. The effect of each parameter on the response signal will be discussed below.

The physical properties of carrier and sample solution are also important. The effect of temperature and viscosity can be summarized by the diffusion coefficient. An increment of its value will be visualized as sharper and narrow peaks, due to a better radial mass distribution. The limit case, infinite radial diffusion, is the basis of the ideal plug-flow pattern flow.

Peak shape is also notoriously influenced by the detector type and the dimension and shape of the detector cell [39–42]. Kinetics phenomena in the flow systems will determine how temporal and spatial concentration gradients enter the flow cell, but the kinetic effects of detection may completely alter these gradients.

Regarding radial mixing, its improvement allows one to obtain a flow pattern more similar to that of plug flow reported by Johnson *et al.* [32] when studying the use of packed loops with different spatial configuration (i.e., "Serpentine II") as a strategy for reducing FIA peak width.

Peaks with shoulders (or humped peaks) have been observed in FIA systems in the absence of chemical reaction, but distortions in the laminar flow pattern tend to smooth them [43]. Nevertheless, in systems where a chemical reaction takes place humped peaks are obtained if the reagent concentration is not in excess with regard to the sample. A limit case of the humped peak is the double peak. In this case the reactant cannot reach the center of the sample plug and the obtained (double) signal is due to the product formation on the head and tail of the sample plug.

Regarding the detection, Růžička and Hansen [16] have suggested that whilst the instantaneous signal of the detector behaves linearly with concentration, there is no difference with the property of the signal used (height or area). Nevertheless, strictly speaking, as also happens in chromatography, only the area of the signal is directly related to the total amount of the analyte injected. Peak height may be used only when the peak profile is not deformed by changing any physical property of the sample.

1.4 The Measurement of Dispersion

The transient signal can be described through different parameters such as peak height (h), time of appearance (t_a), baseline-to-baseline time or peak width (Δt_b), time elapsed between the injection and that of the maximum of the signal (t_r), signal area, and so on. Mostly these parameters cannot by themselves describe the dispersion phenomena and the obtained values are compared with the "ideal" ones. So, these parameters must not be an absolute magnitude since they refer to changes in the mass distribution (redistribution) when compared to the initial condition.

In the next sections, the different parameters able to evaluate dispersion through the characteristics of the transient signal profile will be presented. The employment of these easily calculable parameters is interesting as they allow one to optimize analytical systems in a very practical way.

1.4.1 The Coefficient "D"

The Růžička coefficient of dispersion D is the most popular experimental parameter able to evaluate dispersion in flow systems [27, 44]. Since it is easily calculable, D has been accepted as the way of measuring the degree of dilution of the sample. However, this criterion has been objected to since D involves a punctual definition of dispersion and the main characteristic of the injected pulse is mass redistribution. So, dispersion studies need to be based on a comparison of parameters able to evaluate this distribution. In this way, several papers have focused on study of the peak width rather than D [29, 45] for evaluating dispersion. This will be discussed in the next section.

However, D constitutes a very practical way of comparing different flow systems in relation to their operational variables. Růžička and Hansen proposed a classification of the different flow systems based on D values. This approach allows one to adequate the FI variables to the figures of merit that the analyst wants to optimize.

Růžička and Hansen [27] related the coefficient of dispersion D and the time of residence t_R with the different variables of the system as follows:

$$D = 3.303 \cdot a^{0.496} \cdot L^{0.167} \cdot q^{-0.0206} \tag{6}$$

$$t_R = 1.349 \cdot a^{0.683} \cdot L^{0.801} \cdot q^{-0.977} \tag{7}$$

Vanderslice *et al.* [43] studied the shape of the concentration profiles inside the tube for different elapsed times. Based on these profiles the authors showed that the dispersion coefficient increases with the tube radius. Moreover, it was demonstrated that the asymmetric initial profile becomes quasi-Gaussian at reduced times (τ) close to 1. However, no analytical equation able to show this dependence was presented by the authors.

Narusawa and Miyamae [46–48] employed ZCFIA (zone circulating FIA) and simulation techniques to correlate the system variables with dispersion under conditions of no chemical reaction. The relationships presented by the authors are given in Equation (8):

$$\begin{aligned}
&D_A = 0.045 \cdot L^{1.01} \cdot q^{-1.46} && D_r = 0.349 \cdot L^{0.559} \cdot q^{-0.222} \\
&D_A = 0.076 \cdot t^{1.02} \cdot q^{-0.42} && D_r = 0.449 \cdot t^{0.564} \cdot q^{0.335} \\
&\frac{D_r - 1}{D_A - \theta_t} = 7.5 \cdot L^{-0.45} \cdot q^{1.24} && D_r = 0.388 \cdot L^{0.351} \cdot t^{0.206} \\
& && \frac{D_r - 1}{D_A - \theta_t} = 6.7 \cdot t^{0.75} \cdot q^{-0.48}
\end{aligned} \tag{8}$$

where D_A represents the axial dispersion and D_r is the real radial dispersion (note that it is different from D since the component of radial diffusion is not included in the latter).

Nevertheless, some problems with the experimental set-up, mainly related to the overlap between the head and the coil of the sample plug during the "round trip" of the sample, invalidated the conclusions, as was reported by the same authors later [49].

1.4.2 Peak Width and Time of Appearance

The time of appearance (t_a) is not an estimate of dispersion but it is able to complement the useful information given by the peak width. This last parameter symbolized as Δt_b by Vanderslice *et al.* [50], can be obtained from the transient signal observed in FIA. In some cases, it is useful to employ the peak width expressed as a volume ($\Delta t_b V_b = \Delta t_b \times q$) in order to eliminate the influence of the volumetric flow rate on the residence time of the fluid inside the manifold.

Vanderslice *et al.* reported the dependence of Δt_b on the FI variables. From the numerical integration of the convective-diffusive equation under the conditions imposed by Ananthakrishnan *et al.* [30], the relationships of t_a and Δt_b with the operational variables were obtained as shown in the following equations

$$t_a = \frac{109 \cdot a^2 \cdot D^{0.025}}{f} \left(\frac{L}{\bar{u}}\right)^{1.025} \tag{9}$$

$$\Delta t_b = \frac{35.4 \cdot a^2 \cdot f}{D^{0.36}} \left(\frac{L}{\bar{u}}\right)^{0.64} \tag{10}$$

where f is an adjustment factor which needs to be included since the conditions imposed by Ananthakrishnan *et al.* for solving the convective-diffusive equation are not applicable to the conventional FI systems. It should be noticed that t_a and Δt_b are independent of the loop length "*l*." Even when this is understandable for t_a, since the head of the sample will arrive at the detector at the same time regardless of the length of the injected pulse, it is not the same for Δt_b. In another work [51], the same authors reported the conditions under which the equations presented above are valid.

Regarding the adjustment factor f, Gómez Nieto *et al.* [52] reported that it depends on the flow rate, the length of the manifold and the tubing diameter. Several works were then devoted to the employment of multiple regressions in order to find the experimental coefficients able to fit the experimental variables of the systems with Δt_b or t_a:

$$t_a = 0.898 \cdot a^{0.950} \cdot L^{0.850} \cdot q^{-0.850} \tag{11}$$

$$\Delta t_b = 69.47 \cdot a^{0.293} \cdot L^{0.107} \cdot q^{-1.057} \tag{12}$$

Kempster *et al.* [53] reported the following correlations:

$$\Delta t_b = 48.43 \cdot a^{0.444} \cdot L^{0.282} \cdot q^{-0.893} \tag{13}$$

$$\Delta t_b = 32.33 \cdot a^{0.504} \cdot L^{0.367} \cdot q^{-0.888} \tag{14}$$

Equation (13) was obtained for FI systems with spectrophotometric detection employing a flow cell of 30 µl. Equation (14) was obtained using ICP-OES with a mixing chamber of 300 µl.

Korenaga [45] reported several experiments to correlate t_a and Δt_b with the variables of the system, taking special care to avoid perturbations in the flow pattern. In the case of tube radius (r), the author found a linear relationship between Δt_b and r^2 for $r > 0.33$ mm. For lower values, the relationship was linear with $d^{0.7}$. However, it is difficult to find the reason for these differences since the other experimental variables are not given.

For the reactor length (L), Korenga showed a linear relationship between Δt_b and $L^{0.64}$ which is in agreement with Vanderslice *et al.* (Equation (10)). The same agreement was found for the relationship between Δt_b and q and Δt_b and D (see Eq. (6); Růžička and Hansen [27]).

However, the peak width fails as an estimator of dispersion since dispersion is not only influenced by the length or volume of the injected sample but also by the width of the original sample plug and its deformation while traveling towards the detector. A useful alternative should be the inclusion of the quotient between the final peak width and that of the original sample plug.

1.4.3 Peak Variance and Theoretical Plate Height

According to Tijseen [54], the definitions of dispersion parameters for flow systems are those developed in the field of chromatography for the evaluation of peak broadening. In this way, the variance (σ_{tt}) is proposed as an estimator of dispersion as it is related to the distribution of times of residence of the injected pulse. The peak variance (σ_{tt}) and the theoretical peak height (H), both estimators of dispersion in chromatography, are related by: $H = L\,(\sigma_{tt}/t_m)^2$ (where L is the reactor length and t_m is the time at the peak maximum). When working with Gaussian profiles, such as those obtained in chromatography and in Tijssen's experiments, these estimators of dispersion are proportional to $\Delta t_{1/2.}$

Painton and Mottola [29] reported the relationship between the number of dispersion ($D_N = \mathrm{Pe_L}^{-1}$) and the variance of the curves C vs. t. These relationships are based on the resolution of the convection-diffusion equation under different conditions. The authors found that the variance is proportional to D_N^2.

By employing the exponential modification of a Gaussian function (EMG) [43, 55], Brooks *et al.* [20] evaluated the dependence of the variance on the volumetric flow rate q in a FI system. The peak adjustment through the employment of the equation is only acceptable in systems where a good radial mixture is obtained (use of coiled reactors, low flow rates, long manifolds, etc.).

As stated before, σ_τ and Δt_b fail at the moment of describing dispersion since the size of the initial injected pulse is not taken into account. In other words, if the injection volume is increased under conditions where the injection contribution is not negligible, the variance of the obtained signal will be increased without increasing

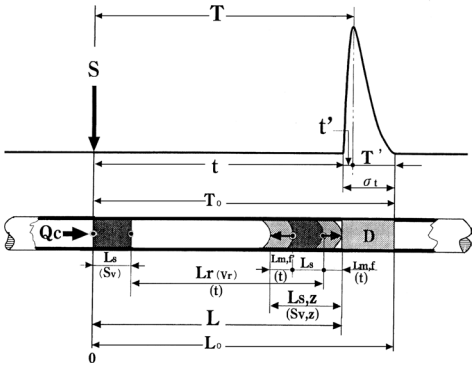

Figure 1.6 Li and Gao Model (Ref. [31]). S = injection point, D = detector, t = time of appearance (t_a), t' = time for the peak ascent, T' = time elapsed between the maximum and the return to the baseline, T_o = total residence time, Q_c = volumetric flow rate of the carrier, Sv = volume of the injected sample, Sv, z = volume of the sample zone, L = reactor length, Ls = sample loop length, Lo = length of the whole manifold, Ls = original length of the injected sample, Ls,z = length of the zone occupied by the injected sample, Lm,f = forward distance in the axial direction (purely dispersive), Lm,b = backward distance in the axial direction (purely dispersive), θ_t = peak width of the injected sample in time units.

dispersion. So, it is convenient to evaluate the different contributions to dispersion in a separate way.

1.4.4 Degree and Intensity of Axial Dispersion

Li and Gao [31] reported two new parameters for the evaluation of dispersion in flow systems. The flow model employed by the authors is shown in Figure 1.6.

The model describes all the parameters that are relevant for a flow system in a very complete way. However, it employs an average of the flow rates developed inside the tube which is not precise since the profile of flow rates in straight tubes is parabolic and the elements of fluid in the central axis travel at twice the average flow rate.

1.4.4.1 Degree of Axial Dispersion

The degree of axial dispersion was defined by Li and Gao as A_D:

$$A_D = \frac{S_{v,z}}{S_v} = \frac{L_{s,z}}{L_s} \cong \frac{\sigma_t}{\theta_t} \tag{15}$$

This adimensional parameter is defined as the quotient between the volume of the sample zone $S_{v,z}$, and the injected volume S_v. $S_{v,z}$, is estimated by assuming that the sample occupies the whole segment $L_{s,z}$. The temporal peak width is obtained by the product of $L_{s,z}$ and the average flow rate, which is not correct. In the case of σ_t (the width of the dispersed sample zone), the flow rate is related to the carrier flow rate

and the "dispersive molecular flow", which is negligible. Regarding the determination of distances in the center of the tube and their conversion into volume, it is not clear. With respect to the relationship with the system variables, they are shown through Equation (16).

$$\begin{aligned} A_D - 1 &= 2\pi \cdot a^2 \cdot t^{0.5} \cdot A_f^{0.5} \cdot S_V^{-1} \\ A_D - 1 &= k_7 \cdot S_V^{-1} \cdot L_R^{\mu_1} \cdot Q_c^{\mu_2} (\mu_1 > 1, \mu_2 < 0) \\ A_D - 1 &= k_8 \cdot S_V^{-1} \cdot t^{\mu_3} \cdot Q_c^{\mu_4} (\mu_3 > 1, \mu_4 > 0) \end{aligned} \tag{16}$$

where A_f is the coefficient for axial dispersion which derives from the concept of model of dispersive axial flow. This model will be presented below. The coefficients k and μ need to be experimentally fitted and their values depend on the tube length and radius, the flow rate and the system configuration.

1.4.4.2 Intensity of the Radial Dispersion

The intensity of the radial dispersion is defined as J_f:

$$J_f = \frac{D}{A_D} = \frac{S_v}{S_{v,z}} \frac{C^0}{C^{max}} \tag{17}$$

where D is the Růžička coefficient of dispersion and A_D the degree of axial dispersion. According to Li and Gao, the larger the J_f value, the higher the radial dispersion of the sample zone and the closer to a square shape. In terms of the signal variance and the signal height, Equation (17) can be written as follows:

$$J_f = \frac{\theta_t}{\sigma_t} \cdot \frac{h_0}{h_{max}} \tag{18}$$

This parameter describes the combined action of sample stretching which is contrasted by the radial mass transfer.

However, when relating J_f with the system variables (Equation (19)), the approach of Li and Gao presents some problems. As an example, the parameter J_f' ("pure intensity of radial dispersion") defined as $J_f' = (D-1) \cdot (A_D - 1)^{-1}$ needs to be equal to J_f^{-1} in order to find consistent relationships with the system variables. These two expressions are not equivalent.

$$\begin{aligned} J_f' &= \frac{D-1}{A_D - 1} \cdot S_V \cdot Q_c^{-1} \\ J_f' &= k_9 \cdot S_V \cdot L_r^{\mu_5} \cdot Q_c^{\mu_6} (\mu_5 < 0, \mu_6 > 0) \\ J_f' &= k_8 \cdot S_V \cdot t^{\mu_7} \cdot Q_c^{\mu_8} (\mu_7 < 0, \mu_8 < 0) \end{aligned} \tag{19}$$

In conclusion, it can be said that even when the parameters for estimating dispersion such as D, peak width and variance fail when performing an exact description of dispersion, they are easily attainable through experimental data and are of great help in developing new analytical methodologies.

1.4.5
Other Approaches to the Measurement of Dispersion

In order to advance in the study of dispersion, Andrade *et al.* [56] reported a new methodology: the integrated conductimetric method (*ICM*) which allows one to follow the mass redistribution process of the injected pulse as a function of time by simply monitoring the electrical conductance (G) of a whole single line system as time elapses. G was measured by placing platinum electrodes in both ends of the manifold. The authors demonstrated that the characteristic profile G vs. time can be assigned to the mass redistribution of the injected pulse along the tube. Later, the same authors [57] proposed a model that fitted the experimental curves with great precision and allowed correlation of the model parameters with the typical FI variables. From these curves it was possible to define a new dispersion descriptor IDQ (integrated dispersion quotient) [57] which was closely related to the Růžička and Hansen dispersion coefficient D. IDQ presented several advantages with respect to D that are summarized as follows: IDQ can be followed continuously with time (D can be evaluated only as a function of t_R), IDQ allows one to perform calculations on a single response curve and, no detector contribution (zero dead volume detection cell) is observed in the measured conductimetric values.

However, as in the case of D, IDQ only takes into account the radial contribution to the dispersion. Another limitation is that, to date, this methodology has only been tested for single line manifolds where no chemical reactions are involved.

1.5
Contribution of the Different Components of a Flow System to Dispersion

A FIA system block diagram is usually composed of four basic elements: a propulsion module, an injection module, the reactor and the detection module. So far, several attempts to study the individual contribution of each module to the overall dispersion have been reported, among these the papers by Johnson *et al.* [32] and Spence and Crouch [34] appear to be the most relevant.

Golay and Atwood [58, 59] applied chromatographic models to FIA and proposed the addition of the variances produced by each section of the FIA system to obtain the global variance of the system. This assumption may be applicable if the peaks are symmetric which, according to the authors, could be reached with at least 30 theoretical plates. However, they demonstrated that such a sum is hard to achieve as any perturbation in the laminar flow means that the sections of the system could not be considered independent of each other (which is the condition for adding the variances), furthermore, in linear systems symmetrical peaks are rarely achieved.

Poppe [60] also showed similarities between chromatography and FIA in terms of peak broadening. It was postulated [55, 61] that the overall broadening may be estimated from the sum of the individual variances due to injection, transport and detection

$$\sigma^2_{\text{Total}} = \sigma^2_{\text{Injection}} + \sigma^2_{\text{Transport}} + \sigma^2_{\text{Detection}} \qquad (20)$$

Note that Equation (20) does not take into account the effects produced by chemical reactions. Detection variance is by far the easiest to minimize and accounts for no more than 10% of the other variances [32]. The importance of these variances lies in the fact that the maximum analytical frequency (f_A) attainable, depends on these variances. Generally speaking, f_A is inversely related to peak broadening [60]. Total variances for Gaussian peaks are easily obtained experimentally, but those for non-Gaussian peaks need to be calculated, as will be mentioned in the next section.

Several studies have been done in order to relate the dispersion coefficient (D) with the individual dispersion coefficients. On one hand Valcárcel and Luque de Castro [62] maintain that D is the addition of all the individual dispersion coefficients of the system, that is, injection, transport and detection, while, on the other hand, Růžička and Hansen [16] propose that D is the result of the product of all individual dispersion coefficients. The Růžička and Hansen approach is based on the idea that the signal decays a certain degree while passing through each section of the system, hence the overall decay should be modeled as the product of all individual decays.Valcárcel and Luque de Castro do not explain the fundamentals of their approach.

Spence and Crouch [34], based on the theory of the independent contribution of the individual variances to the global variance described by Equation (20), analyzed the contribution to dispersion arising from the different components of a conventional FIA system and a capillary FIA system by varying the dimensions of the detection cell, the length of the FIA conduit and the injection volumes. They were able to obtain estimates of the contribution of each component for a given linear flow rate. Linear regressions between the global variance and reactor length, injection volume and flow cell volume were established, and the authors assumed a linear relationship between these variables and the variances of each system. As was shown in the previous section, these relationships are not linear (i.e., detection cell variance is proportional to the volume of the cell squared), but the regression coefficients presented were very close to 1000. The authors concluded that, for a conventional FIA system, the contribution to the global variance due to the detection is about 6%, while for a capillary FIA this contribution rises to 40%. Similarly, the injector contributes 40 and 28%, respectively, and the reactor contributes 60 and 32%, respectively. The authors consider that the main contribution is due to the flow cell and this assumption may not be correct, as was mentioned previously.

A deeper analysis of the data presented in the paper shows several facts not considered by the authors:

1. The slope of the regression of the global variance vs. cell volume for the capillary system is four times larger than for the conventional FIA system, indicating the importance of the cell volume in capillary systems. As the linear flow rate (u) was kept constant in both systems, this enhanced dependence of the variance on the cell volume should undoubtedly be related to the lower volumetric flow rate (q) in capillary systems, which in turn produces a larger residence time inside the flow cell, and hence a larger variance.

2. The analysis of the dependence of the variance on the reactor length (L) reveals that the slope for capillary systems is half that of a conventional system, indicating a

Table 1.2 Constants for Equation (21).

	Capillary system	Conventional system
k_1 [$s^2\,cm^{-1}$]	0.60	1.39
k_2 [$s^2\,\mu l^{-1}$]	6.39	8.39
k_3 [$s^2\,\mu l^{-1}$]	80.9	23.1

smaller variance for the former system or, which is the same, that the sample "stretches" less in capillary systems.

3. The contribution of the injector to global dispersion is more relevant in conventional systems than in capillary systems. This may be explained by considering that in both cases the injection is done "in time" and the contribution of the injection is influenced by the transport type, and hence the dispersion is smaller as the tube radius is diminished.

4. The global variance for capillary systems is only 75% of the global variance of conventional systems, meaning an increase in peak height (lowering the detection limit) and a decrease in peak width (increasing the analysis frequency).

The expression for the global variance as a result of the regression analysis may be written as:

$$\sigma^2_{peak} = k_1 \cdot L + k_2 \cdot S_V + k_3 \cdot V_{cell} \qquad (21)$$

where each term represents the variance of each component in Equation (20). In Table 1.2, the values for each constant are the slopes of the regression graphs and the units should be coherent with the units used at the time the data are adjusted.

Equation (21) may be used to evaluate the result of the global variance produced modifying some of the operational variables of the system. It must be emphasized that the injection variance cannot be minimized as this would imply diminishing the injection volume which in turn would affect the signal height if the cell volume is not reduced consequently.

Unfortunately it is not possible to estimate the error in Equation (21) as the authors have not reported the regression errors for the slopes (they do report intercept errors). However, as the regression coefficients reported are close to 1, it would be expected that this equation should be valid for the range of values explored for each variable: L (50–400 cm), S_V (0.72–1.25 µl), V_{cell} (0.325–1.14 µl).

1.5.1 Injection

The injection contribution and its variance have been studied by several authors and it was concluded that the way in which the injection is carried out has a great influence on the dispersive process and on the profile obtained and that this influence tends to grow as the injection volume increases [32, 35, 36, 61, 63].

As was mentioned before, the most common injection technique consists in emptying a loop filled with sample into a carrier stream. The usual FIA conditions impose a parabolic and laminar flow profile that provokes a deformation of the injected plug which, in turn, leads to an increase in dispersion. Johnson *et al.* [32] have reported some alternatives to diminish the deformation of the injected plug by using packed reactors and "serpentine" reactors to obtain a plug type injection.

Time injection, in which the loop is not emptied completely, is an alternative technique that allows reduction of the peak width [63] as only the first portion of the sample is injected, eliminating "tailing." One of the drawbacks of this type of injection lies in the pressure changes that might not be reproducible, thus affecting the overall reproducibility of the system.

Injection variances obtained for time injection and loop injection were analyzed by Reijn *et al.* [61]. They found that the values of the variance obtained in each case were related to the injection ratio squared.

1.5.2 Detection

The contribution to the dispersion arising from the detection system may be described as the result of several individual contributions associated with minor components of the detection system: connecting conduits, geometry of the cell, response time of the detection cell [42], and so on. Poppe [60] analyzed the detection variance, expressed in volume terms, as:

$$\sigma^2_{\mathrm{Vol,detection}} = \sigma^2_{\mathrm{Vol,transp}} + \sigma^2_{\mathrm{Vol,cell}} + \sigma^2_{\mathrm{Vol,resp.time}} \tag{22}$$

As it is not possible to know the flow pattern generated inside a flow cell, the contribution of cell geometry to the variance is very difficult to predict. Poppe estimated that for a flow cell of V_{cell} volume, the volumetric standard deviation ($\sigma_{\mathrm{Vol,cell}}$) may vary between 0.29 and 1 times the cell volume.

$$0.29^2 S_V^2 < \sigma^2_{\mathrm{Vol,cell}} < S_V^2 \tag{23}$$

This estimate arises after considering two extreme cases: (i) the cell behaves as an ideal mixing chamber whose washing follows an exponential decay (in this case the standard deviation could be deduced to be 0.29 V_{cell}) or (ii) the flow is "plug type" inside the cell and in this case the standard deviation is equal to the cell volume. It follows that when the injected volume is similar to the cell volume, one could expect some errors in the evaluation of the effects of the different variables on the dispersion, as the cell would act as a mixing chamber.

A dispersion model should be used to estimate the contribution due to transport phenomena (see below) as this model adjusts best to the environmental conditions of system conduits. Volumetric variance due to response time is equal to the flow rate multiplied by the time constant of the detector [60]. Taking into account these variables, it may be deduced that volume peak broadening due to detection increases with flow rate as, excluding the variance due the cell geometry, the other variances depend on "u."

1.5.3 Transport: Different Models

Several models have been generated in order to find correlations among the different system variables. The purpose of this section is to give a global view of those models and their scope, as well as an evaluation of their advantages and drawbacks. If the reader is interested in this field, we recommend some reviews on the subject [64, 65].

1.5.3.1 Descriptive Models or "Black Boxes"

Experimental results may be very well represented by descriptive models, but these models usually do not provide a better understanding of the chemical and physical mechanisms which gave rise to such results. In this sense, systems are considered as "black boxes" where the model tries to correlate the results to the entrance parameters.

The tank-in-series model is applied in chemical engineering as a deterministic model for dispersion in big reactors, and although FIA conditions differ from these environmental variables, Růžička and Hansen [27] used this model when dealing with recommendations for optimizing FIA systems. This approach has been fully explained and analyzed by the authors and will not be discussed here.

On the other hand, several authors have depicted the FIA peak as a Gaussian peak modified by an exponential function (EMG). This was first introduced by Foley and Dorsey [38] and applied to a number of FIA systems [66]. Although these models do not describe the dispersive processes, they are useful for estimating peak parameters which is necessary when comparing and evaluating different systems. Later, peak parameters, known as statistical momenta, have gained importance after the studies of Ramsing *et al.* [67] and Reijn *et al.* [68], as they could be used to evaluate any profile.

Regression analysis has been widely used in FIA, and the dependence of the dispersion coefficient D, peak width, appearance time, and so on, on the different FIA system variables has been reported [64] using least squares methods. The validity of these equations is restricted to the systems for which they were deduced as the influence of the component characteristics on the responses makes generalization impossible [20].

Artificial learning models based on neuronal networks have been used recently to model FIA systems [69]. This method is based on generating a network of processing units (neurons), each neuron receives a certain number of input signals and, according to a previously established priority order, the neuron is caused to emit an output signal. The priority is established through a set of experiments in which the neurons "learn" how to behave. Once the learning is complete the system might be used in a predictive way, the capacity of prediction being proportional to the number of neurons. There is a natural limit to the number of neurons which is set by the increase in the capacity of the neurons for learning "noise." The major drawback of this approach is the need for large processing capacity.

1.5.3.2 Deterministic Models: Dispersive Models and Tank-in-Series Model

Deterministic models are those models in which the global behavior of a system is followed through numeric relationships between different parameters. The value

assigned to each parameter is imposed by the environmental condition of the system. Most of the systems analyzed consider that the dispersion only takes place in the reactor.

Dispersive models take into account the variations in behavior of the system in each region, considering both diffusive and convective contributions as a function of the environmental conditions of the system. They are mainly based on the diffusion-convection equation or on phenomenological modifications of it.

Applied to cylindrical tubes, the dispersive model is depicted by the differential equation which shows the changes in concentration of a substance as a function of time along the system length:

$$\frac{\partial C}{\partial t} + u(r) \cdot \frac{\partial C}{\partial z} = \frac{1}{r} \cdot \frac{\partial}{\partial r}\left(r \cdot D_r \cdot \frac{\partial C}{\partial r}\right) + \frac{\partial}{\partial z}\left(D_L \cdot \frac{\partial C}{\partial z}\right) + s \tag{24}$$

where $u(r)$ is the velocity profile in the tube, D_L the axial dispersion coefficient (which in turn depends on r), D_r the radial dispersion coefficient (which is a function of z) and s accounts for the kinetic contribution due to the appearance or consumption of substance as a result of a chemical reaction.

This model has been used only twice for FIA: the uniform dispersion model and the axially dispersed plug flow model. In the former the following assumptions are made: (i) a parabolic velocity profile is developed, (ii) phenomenological dispersion coefficients (axial D_L and radial D_r) are equal and are also equal to D_m the diffusion coefficient of the substance. In the second model, a uniform velocity profile is assumed, and hence it is assumed that only axial diffusion is possible.

Uniform Dispersion Model This model is based on Equation (24), taking into account the actual velocity profile inside the conduit, which depends on the geometry of the manifold. It is assumed that axial and radial dispersion coefficients are constant along the system and equal (or proportional) to the molecular diffusion coefficient. Equation (24) can then be written as:

$$\frac{\partial C}{\partial t} = \frac{D_r}{r}\frac{\partial}{\partial r}\left(r\frac{\partial C}{\partial r}\right) + D_L\frac{\partial^2 C}{\partial z^2} - u(r) \cdot \frac{\partial C}{\partial z} + s \tag{25}$$

As was mentioned before, in the conditions usually employed in FIA, the flow pattern inside the tubes is laminar ($Re < 2300$), the velocity profile for straight tubes is parabolic and this situation is known as Poiseuille–Hagen flow. In this particular case Equation (25) can be written as:

$$\frac{\partial C}{\partial t} = D_m\left(\frac{1}{r}\frac{\partial C}{\partial r} + \frac{\partial^2 C}{\partial r^2} + \frac{\partial^2 C}{\partial z^2}\right) - 2\bar{u}\left(1 - \frac{r^2}{a^2}\right)\frac{\partial C}{\partial z} + s \tag{26}$$

where $\bar{u}$ is the fluid mean velocity and a is the tube radius.

Axially Dispersed Plug Flow Model If a uniform velocity profile is assumed, and hence there is no radial variation of velocities:

$$\frac{\partial C}{\partial t} = \frac{D_r}{r}\frac{\partial}{\partial r}\left(r\frac{\partial C}{\partial r}\right) + D_L\frac{\partial^2 C}{\partial z^2} - u\frac{\partial C}{\partial z} + s \tag{27}$$

where u is independent of r and equal to the mean fluid velocity ($\bar{u}$). No radial concentration gradient should be created under this assumption and the term which accounts for this diffusion is logically negligible. This leads to the model known as axially dispersed plug flow.

$$\frac{\partial C}{\partial t} = D_L \frac{\partial^2 C}{\partial z^2} - \bar{u}\frac{\partial C}{\partial z} + s \tag{28}$$

Equation (28) may also be written as:

$$\frac{\partial C}{\partial t} + \frac{\bar{u}}{L} \cdot \left(\frac{\partial C}{\partial z'}\right) = \frac{D_m}{L^2} \cdot \left(\frac{\partial^2 C}{\partial z'^2}\right) \tag{29}$$

where z' is a reduced dimensionless expression for the distance, $z' = z \cdot L^{-1}$.

Considering a delta injection, waterproof tube walls and an endless tube, the variance of the concentration profile at time t and distance L from the origin is:

$$\sigma_t^2 = \frac{2 \cdot D_L \cdot L}{\bar{u}^3} \tag{30}$$

Although this model has been used in several fields, such as chemical engineering, chromatography and even FIA, its application is valid only in those systems where the flow pattern does not generate a radial concentration gradient, which is not the case for FIA where the parabolic flow profile generates a radial gradient which is not negligible.

Tanks-in-Series Model The tanks-in-series model [27, 70] assumes that point to point variations within the FIA system are very small, and hence the system may be considered as homogeneous regarding its properties and dependent variables. In this case, a complete mix between the injector and the detector is considered, being either hypothetical (Tyson and Iris [71]) or obtained through the use of some kind of mixing chamber (Pungor *et al.* [22]). This model is similar to that used in chromatography (ETPH) as it assumes N ideal mixing stages. Nevertheless, it is necessary to stress, that chromatographic peak broadening is the result of dynamic processes caused by the column packing which are absent in most FIA applications.

The equations used are based on residence time curves which may be found in most Chemical Engineering books [26] and will not be discussed here. The model description and the main conclusions are reported elsewhere (see [72]).

However, it should be noticed that experimental peak profiles, when compared to predicted profiles, show a good match in the ascending and descending portions of the curve but not in the maximum nor in the shape. It might be concluded that this model, although simple, does not allow a deep knowledge of the processes occurring, and hence its use for modeling systems without a mixing chamber is limited. On the contrary, this model predicts very well those systems in which a mixing chamber is used, or if single bead string reactors or gradient chambers [64], such as those used in FIA titrations, are present.

1.5.4 Probabilistic Models

1.5.4.1 Random Walk

Random walk has been widely employed in physicochemical studies in order to explain and predict the effect of diffusion of the solutes [19]. The model involves multiple steps, the direction of each step being independent of the direction of the previous stage. Generally, an origin is fixed and then steps of a given length are given in the x and y directions:

$$(\Delta x_1, \Delta y_1), (\Delta x_2, \Delta y_2), (\Delta x_3, \Delta y_3), \ldots, (\Delta x_N, \Delta y_N) \tag{31}$$

where N is the total number of steps and the distance traveled since the initial point ($\boldsymbol{R}$) is given by:

$$\begin{aligned} R^2 &= (\Delta x_1 + \Delta x_2 + \ldots + \Delta x_n)^2 + (\Delta y_1 + \Delta y_2 + \ldots + \Delta y_n)^2 \\ R^2 &= \Delta x_1^2 + \Delta x_2^2 + \ldots + \Delta x_N^2 + 2\Delta x_1 \Delta x_2 + 2\Delta x_1 \Delta x_3 + \ldots \end{aligned} \tag{32}$$

The expression above is general and independent of the direction of the *walk* since the chance for moving back and forward is the same. In this way, on average, for a great number of steps the crossed terms of Equation (32) are cancelled giving the following expression:

$$\begin{aligned} R^2 &\cong \Delta x_1^2 + \Delta x_2^2 + \ldots + \Delta x_N^2 + \Delta y_1^2 + \Delta y_2^2 + \ldots + \Delta y_N^2 \\ R^2 &\cong N\langle r^2 \rangle \\ R &\cong \sqrt{N} r_{\mathrm{rms}} \end{aligned} \tag{33}$$

where r_{rms} is the root mean squared step size. This result can be extended to an axis of three coordinates with the same assumption. In agreement with the equation above, even if the average distance of the total walk is $N \cdot r_{\mathrm{rms}}$, the distance from the initial point is $r_{\mathrm{rms}} \cdot N^{0.5}$.

Betteridge *et al.* [73] were pioneers in the application of this model since they studied the effect of different variables on the signal given by a single line FI system where the injection of a discrete number of molecules was simulated. This approach was then extended to confluence FI systems [74] and to SIA [4]. Later, Wentzell *et al.* [75] studied different FI systems without chemical reaction where different flow profiles and conditions of infinite radial diffusion were incorporated.

Since this model is based on the fate of each molecule, it is easy to simulate the effect of sample size, physical dispersion and chemical reaction. The obtained results show good agreement with reported experimental studies in systems *without chemical reaction*.

The random walk simulation has a great capacity for predicting the shape of the curve that should be obtained by monitoring the whole FI system in a longitudinal way. The equations employed in the simulation will not be presented here. However, if the reader needs a deeper knowledge of this issue, several papers can be consulted [19, 73–77].

Regarding the advantages of the random walk modem, they were reported by Kolev [64] and can be summarized as follows: (i) ease of observation of the influence of different flow types, (ii) mathematical and computational simplicity, (iii) good graphic visualization of the results. Amongst the disadvantages, the method has shown certain problems with quantitative prediction which can be improved by a longer computational time.

1.6 Design Equations

Reijn *et al*. [78] proposed design equations to maximize the frequency of analysis and minimize the consumption of reactants for linear systems in coiled and single bead string reactors. Tijssen [54] proposed design equations for systems with coiled reactors, as shown previously. Other design equations based on the tanks-in-series model were provided by Růžička *et al*. These design equations fail for low dispersion cases [79]. Other reported equations will not be presented here as they only work in very specific systems.

The following section aims to provide evidence for the effect of different operational variables on the obtained signal. In order to do this, a $CoSO_4$ solution with an absorbance value equal to 0.341 of absorbance was prepared. Double deionized water (DDW) was used as carrier, and the absorbance was monitored at the maximum of the cobalt–water complex ($\lambda_{máx} = 525$ nm). Different flow rates and tubes of different radius, length and geometry were used [77, 80].

1.6.1 Influence of the Different System Variables

1.6.1.1 Reactor Length

In all cases, and for any reactor configuration, an increase in the traveled distance, providing that all the other variables stay unchanged, means an increase in the dispersion of the sample (peaks tend to be shorter and wider, Figure 1.7).

1.6.1.2 Geometric Configuration

The influence of the spatial configuration of the reactor depends on the other system variables. The more the contribution of the dispersion due to transport to the total dispersion and the more efficient the secondary profiles production, the more notorious will be the differences on dispersion found between straight and coiled reactors.

Regarding this last factor, the arising of secondary flows will be more evident as reactor length and carrier linear rate increase. This behavior is found also in other types of reactor that want to maximize secondary flow production, like knotted reactors in which the flow direction changes successively, favoring the mass radial transfer. The more often this event occurs, the more uniform the rate distribution will be, as well as the similarity with the plug-type flow [16, 81]. A major efficiency in the minimization of the dispersion is reached when knotted reactors (periodic or random

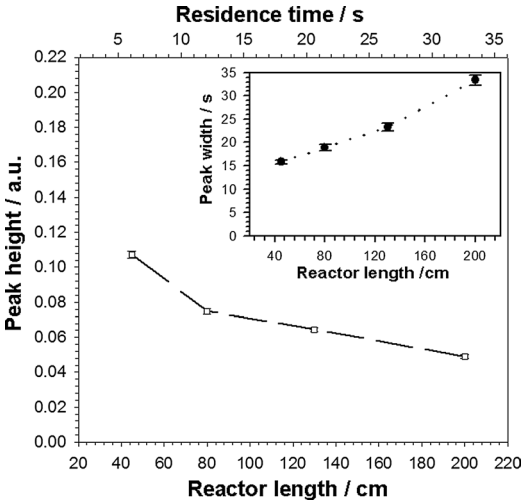

Figure 1.7 Influence of the reactor length on dispersion.

knots) are used instead of coils. This is due to the frequent changes in the direction of flow: in the knotted reactors this change is periodic, whereas reactors with irregular knots produce an odd disturbance of the flow profile [16].

1.6.1.3 **Flow Rate**

The dependence of the different descriptors, mainly D, on the flow rate seems to be unclear. Li and Ma [82] studied this dependence by employing coiled reactors in the system but, unfortunately, in this kind of geometry, the capability to reduce dispersion is, precisely, a function of the flow rate. The authors found a maximum in the D vs. q plot with medium flow rates. This maximum was found to be independent of the length and diameter of the tube, as well as of the injection volume. However, it showed some relation to the substance diffusion coefficient (the value of q in the maximum is smaller as this coefficient increases).

On the other hand, in a previous work, Stone and Tyson [83] analyzed the different factors that affect dispersion in flow systems, including flow rate, and found that, for short tubes, dispersion decreases monotoneously as the flow rate increases. Nevertheless, as tube length increases, a maximum in the D vs. q plot can be seen for low flow rates. The q value for which this maximum appears depends on reactor dimensions, in contrast with Li and Ma's observations [82] for exactly the same systems. In spite of this, it is worth analyzing the trend of the D vs. q plot.

The differences found in classic bibliography about the dependence of D on q can be explained in terms of the point at which the maximum appears. As an example, the experimental conditions used by Růžička and Hansen [16] who support that D increases as q increases, are located before this maximum, while those used by Valcárcel and Luque de Castro [62], who support that D decreases as q increases, are located after it.

From the simplest point of view, if the sample goes through a plug-type flow regime, it would have the same mass radial distribution as that of injection at any time during its travel. These conditions can be approached in FIA at very (impractical) low flow rates. Then, as the flow rate increases, the mass radial distribution contributes to the increase in the coefficient D. Nevertheless, at greater flow rates, where the main dispersion source is convection, the coefficient D decreases again (assuming that the instrumental time of response is null). In this way, the observations made by the authors are valid, and the difference in their conclusions can be ascribed to a misinterpretation of the different experimental conditions.

Stone and Tyson, and Li and Ma, were correct when they realized that q and L are factors that affect the residence time and, therefore, comparison of the different systems becomes difficult when q and L are modified due to the different contribution of the convective and diffusive processes. For example, for short manifolds and high rates, the contribution is only convective. Nevertheless, if, keeping q constant, L increases, the influence of the diffusive process increases. If a plot of this, as a function of the residence time, is made (Figure 1.8), the result is an increase in D as t_R increases. This profile is much influenced by the flow cell used, in certain cases, D and q are found to be independent for some values of q [83, 84], depending on the length of the tube and the volume of the flow cell [83].

The maximum value on the D vs. q chart is due, then, to the existing dependence between the residence time of the solute and the flow rate. The residence time is inversely proportional to q and it is commonly calculated [16] as the ratio of the reactor length and the average flow rate ($t_R \approx L \times q^{-1}$). Nevertheless, Li and Ma found that actually t_R is proportional to q^{-k}, and that k is less than 1 for low flow rates and greater than 1 for high rates. According to the theoretical expression of D given by Růžička and Hansen [16], it can be said that D is proportional to $(t_R \cdot q)^{1/2}$. Therefore, if k is less than 1, the t_R value is a little bigger than expected if q^{-1} is taken into account and D increases as q increases. The opposite is observed if k is greater than 1.

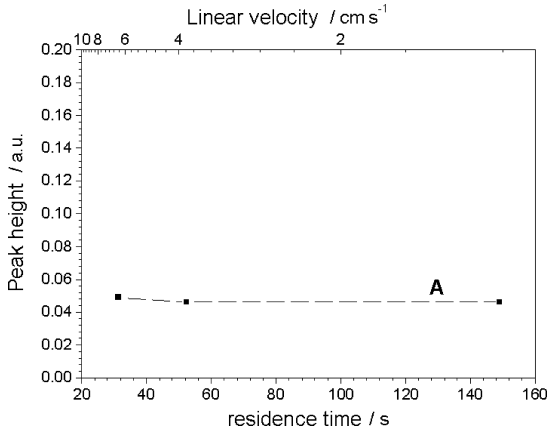

Figure 1.8 Effect of the flow rate on dispersion.

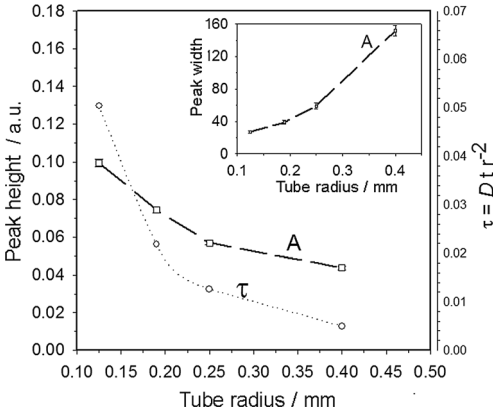

Figure 1.9 Effect of the tube radius on dispersion.

For the case of the peak width, decreasing hyperbolas described by negative exponents of q are obtained as a function of q. The coefficients that describe these hyperbolas depend on the reactor spatial configuration, being smaller in absolute value for the case of coils than for straight tubes. As long as the flow rate decreases, this difference is less noticeable.

1.6.1.4 Tube Radius

As shown in Figure 1.9 and the different published works on this issue [45, 82, 83], as the tube radius decreases, D and the peak width also decrease, at a constant linear flow rate (u). However, it is necessary to say that certain studies, such as Li and Ma's [82], were performed keeping the volumetric flow (q) constant instead of the linear flow rate (u). Thus, the decrease in dispersion is mainly due to a lower t_R for the tubes of smaller diameter, the contribution of the radial mass being less significant in these cases. This contribution can be observed in terms of τ, where the greater diffusive contribution is shown as an increase in the reduced time value.

Figure 1.9 (inset) shows the obtained peak width as a function of the tube radius. There is an important factor to be considered when these plots are compared keeping linear flow rates (u) constant, using different tube radius. In these cases the employed volumetric flow rate (q) changes, and so does the flow rate inside the flow cell, making the comparison unfair. Thus, the real peak width value should be corrected by the average residence time inside the cell, which is a factor of very low importance for high rates and tubes of large radius, but is relevant for low rates and tubes of small radius. As can be seen in Figure 1.9, the peak width increases with the tube radius (a). When a decreases, the signal gets taller and the peak gets narrower, which implies a relatively greater analysis frequency gain rather than a gain in sensitivity.

1.6.1.5 Injection Volume

The dependence of the transient signal on the injection volume S_V has been shown by Růžička and Hansen [16]. This dependence is key to the control of the dispersion, since it affects significantly the signal, the residence time and, for large injection

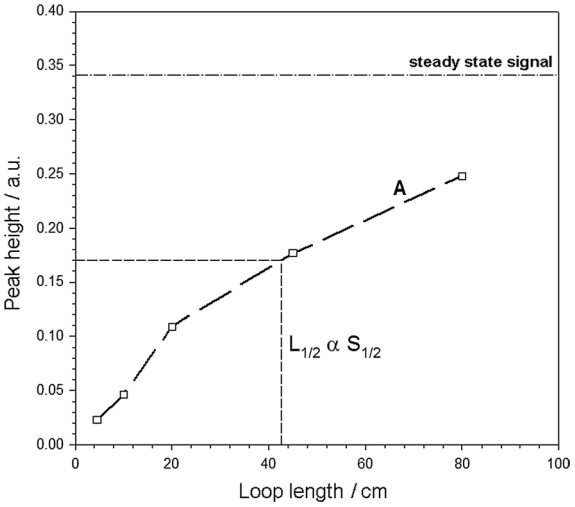

Figure 1.10 Effect of loop length on dispersion.

volumes, the peak width. When the signal height as a function of the injection volume (or of the length of the loop) is plotted, the curves shown in Figure 1.10 are obtained. This dependence has been described [16] through the following phenomenological equation:

$$\frac{1}{D^{\max}} = \frac{C^{\max}}{C^0} = 1 - e^{-K \cdot S_V} = 1 - e^{-0.693 \frac{S_V}{S_{1/2}}} \tag{34}$$

The parameter $S_{1/2}$, (the required sample volume to reach a half of the signal of the stationary state or $D = 2$) is useful to define the performance of a system as it depends on different variables of the system. The coefficient K is inversely related to $S_{1/2}$ and indicates how steep is the slope of the curve shown in Figure 1.10.

In the ideal case of a system without dispersion, the injection volume does not influence the signal height, but has a direct relation to its width. This is true only when the injection volume is bigger than the cell volume. In this ideal situation, K should tend to infinity and D, as expected, should be equal to 1.

Equation (34) can be linearized [83], obtaining:

$$\ln\left(1 - \frac{1}{D^{\max}}\right) = -\frac{0.693}{S_{1/2}} S_V \tag{35}$$

With this, $S_{1/2}$ can be obtained through the slope of the curve that better fits this dependence.

When evaluating this parameter in real systems, care must be taken, especially with small tube radius where the influence of any dead volume inside the system is notorious. For the case of injection volumes that generate peak heights statistically non-different from the signal of the stationary condition, fitting of Equation (35) will not be good as it predicts that the signal is reachable only for S_V tending to infinite.

Stone and Tyson [83] show that D has similar values in systems that keep the relation between the injection volume and the reactor volume constant, without considering the tube radius. In contrast, there is a strong reduction in $S_{1/2}$ if the tube's radius gets smaller.

Moreover, these authors find the major symmetry of the transient signal with temporal injections rather than slug-type ones. They also show the influence of the injection "mode" which becomes more relevant as long as the influence of the injection on the global dispersion increases (i.e., systems where the loop length is close to the reactor length). In these cases, the dispersion due to transport is not relevant.

Regarding the dependence of the peak width on the injection volume, it has been discussed that it is minimal if the length of the loop is less than 20% of the reactor length. This is because, in these cases, the transport contribution to dispersion is greater than the injection contribution. Nevertheless, the general trend is that when the injected volume increases, the width of the obtained peak also increases.

Taking into account Stone and Tyson's considerations about the equality in D values observed in those systems where the relationship between the injection volume and the reactor volume is the same, Equation (34) can be re-written as follows:

$$\frac{1}{D^{\max}} = 1 - e^{-K\frac{S_V}{V_{reactor}}} = 1 - e^{-\left[\frac{0.693}{\left(\frac{l}{L}\right)_{1/2}} \cdot \frac{l}{L}\right]} \tag{36}$$

where $\left(\frac{l}{L}\right)_{1/2}$ is the length ratio for D equal to 2, and it should be independent of tube radius in order to fulfill the presumptions of Stone and Tyson. This expression may be used as a design equation: the loop to reactor length ratio is chosen so as to obtain the most wanted D value (i.e., based on the desired sensitivity) and the flow rate is chosen to obtain a given residence time (i.e., based on the reaction time).

1.6.2 Optimization of Flow Systems

This way of optimization looks for the maximum utilization of the flow secondary profiles, considering the set of instruments commonly available in FIA. It is based on the work of Reijn *et al.* [85] and Tijssen [54].

The use of a peristaltic pump in FIA imposes limitations to the range of flows that can be used and to the system back pressure that the pump can support. The minimum residence time in a system regarding these limitations can be calculated as follows:

$$t_p = \frac{8 \cdot L^2 \eta}{\Delta p \cdot a^2} \tag{37}$$

t_p is known as "limited time by pressure." The maximum backpressure (Δp) for a peristaltic pump is about 5 bar, while for a plunger pump in liquid chromatography it is about 400 bar. In coiled tubes, the existence of secondary flows causes an increase in the axial pressure, although for De less than 25 the excess of pressure is less than 10%,

compared with a straight tube. Although it can be thought that the sophistication of the pump system is a way to increase the maximum backpressure, it should be noticed that for an increase of 10 in Δp, the minimum radius decreases [85] by a factor of 1.47, which is not a great improvement considering the increment in the instrumental costs.

Another limitation due to the maximum flow that the propulsion system can provide is known as "limitation by flow." For this case the minimum obtainable residence time is calculated by:

$$t_F = \frac{L \cdot \pi \cdot a^2}{q_{max}} \tag{38}$$

Considering a peristaltic pump, the maximum flow that can be supplied is about $30\,cm^3\,min^{-1}$.

The analytical throughput (f_A) is determined by the peak width which, in Taylor's conditions, can be written as:

$$f_A = \frac{60}{6 \cdot \sigma_t} = 10\sqrt{\frac{24 \cdot D_m}{a^2 \cdot t}} = \frac{49}{a}\sqrt{\frac{D_m}{t}} (\text{in } min^{-1}) \tag{39}$$

where t is the residence time in the system. As can be seen, the frequency of analysis should be independent of variables such as flow (q), pressure fall (Δp) and reactor length (L), although these variables impose limits to the working a values and the reachable t values.

The carrier consumption per peak (F, in cm^3) [54] can be obtained as follows:

$$F = q \cdot 6\sigma_t = 6\pi a^2 \bar{u}\sqrt{\frac{a^2 t}{24 \cdot D_m}} = \frac{3\pi}{4} a^4 \sqrt{\frac{\Delta p}{\eta D_m}} \qquad \left(\frac{\Delta p}{L} = \frac{8\bar{u}\eta}{a^2}\right) \tag{40}$$

Regarding the system optimization, the data obtained by Tijssen can be presented in a practical way in Figure 1.11. Taking into account the desired analytical frequency and

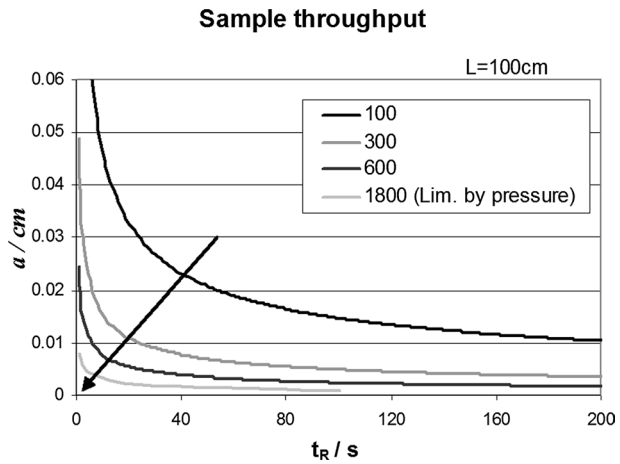

Figure 1.11 Analytical frequency as a function of t_R in FIA conditions.

the residence time, the required diameter of the tube can be obtained. With this, for a given analytical frequency, the greater the desired residence time, the smaller should be the tube radius.

Regarding the pressure fall that the peristaltic bomb can support (about 4 bar) the maximum reachable frequency of analysis in FIA is, theoretically, about 1800 peaks per hour.

For coiled tubes, the decrease in the theoretical plate height improves the analytical frequency, and the carrier consumption per peak decreases. Nevertheless, high flow rates are necessary to obtain big differences. As F, f_A, and H are direct functions of σ_t, it can be seen that the improvement in the height of the theoretical plate for coils compared to straight tubes (H/H_0, where the subscript "0" is used for straight tubes) is directly related to F and f_A through:

$$\sqrt{\frac{H}{H_o}} = \frac{S_o}{S} = \frac{f_A}{f_{A_o}} \tag{41}$$

For example, to double the analytical frequency, $(H/H_0)^{1/2}$ should be equal to $^1/_2$, which is obtainable with a De^2Sc greater than 10^4. In practice, values of De^2Sc close to 10^8 can be obtained, which implies a frequency of about 100 times greater in coil tubes. Nevertheless, this is valid only when transport is the main contributor to the total dispersion.

It is now time to think how to proceed to choose the optimal conditions for a system when a certain residence time is required. If systems with a chemical reaction are analyzed, the residence time only modifies the degree of reaction.

The idea is, then, to calculate the maximum value of De^2Sc to maximize the effects of the secondary flow, once the reaction time is selected. To do this it is necessary to work with flow and pressure fall as large as possible, and so it is only left to set the residence time and take into account the limitations of the maximum pressure fall and the flow rate obtainable to determine the maximum De^2Sc. It is obvious that the desired residence time should be reachable by considering the maximum pressure fall and the maximum flow. So, the following equations can be derived:

$$t_R = t_p = \frac{8 \cdot L^2 \eta}{\Delta p \cdot a^2} = t_F = \frac{L \cdot \pi \cdot a^2}{q_{max}}$$

$$L_{optimo} = \sqrt[3]{\frac{\Delta p_{max} \cdot q_{max} \cdot t_R^2}{8 \cdot \eta \cdot \pi}} \tag{42}$$

$$a_{optimo} = \sqrt{\frac{q_{max} \cdot t_R}{\pi \cdot L_{optimo}}}$$

Once these values are obtained, H/H_0 can be evaluated calculating De^2Sc (for a given λ) through the formula given above. Figure 1.12 shows an experimental adjustment done with the data presented by Tijssen in order to make this calculation easier and to obtain an estimate of the obtainable improvement in coiled tubes using peristaltic pumps instead of plunger ones as Tijssen suggested.

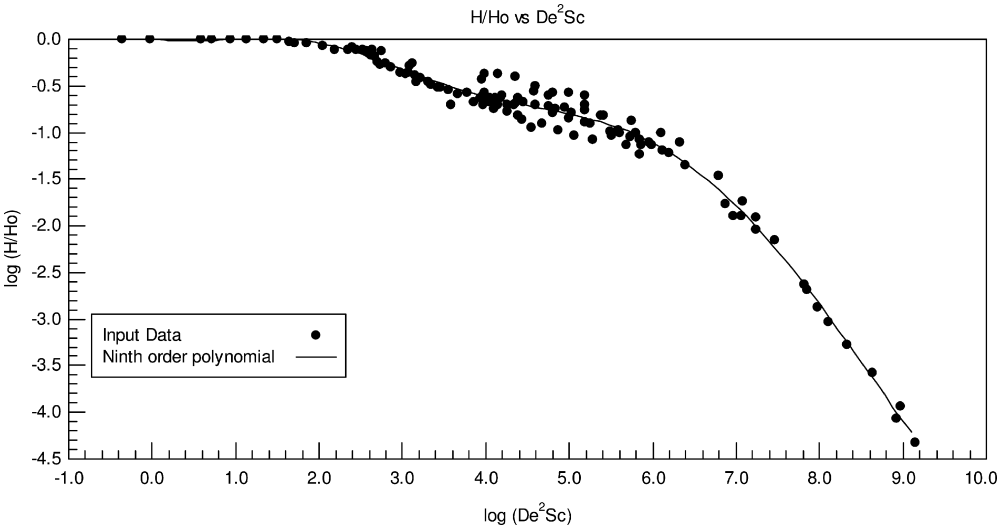

Figure 1.12 H/H_0 relation adjustment as a function of De^2Sc.

Once H/H_0 is known, it is possible to calculate f_A and F. Table 1.3 shows the calculated values with Tijssen's conditions and under other proposed conditions.

It can be concluded from these data that the best results are those where the maximum flow and pressure fall were used. The calculation for the reachable conditions using conventional FIA instrumentation shows a great improvement in the frequency of analysis (about 5 times greater), but the improvement in reactants consumption per peak was of less importance, about only 3 times less.

As the product De^2Sc increases when the tube length increases or the radius decreases, a compromise is reached, in which maximum values for reactor length (L) and tubes not too wide (0.1–0.5 mm i.d.) have to be obtained. One reason for this is

Table 1.3 Optimum operational conditions for different systems.

p_{max}	bar	400	400	80	4
$q_{máx}$	$cm^3\,s^{-1}$	0.5	0.5	0.1	0.5
t_R	s	10	100	10	60
L	Cm	4301	19 965	1471	3060
A	Cm	0.0192	0.0282	0.0147	0.0559
De^2Sc		1.96×10^8	9.08×10^7	1.34×10^7	2.32×10^7
H/H_0		6.36×10^{-4}	1.62×10^{-3}	1.25×10^{-2}	7.32×10^{-3}
$(H/H_0)^{-1/2}$ (coil/recto improvement)		39.7	24.8	9.4	11.7
f_{A_0}	peaks min^{-1}	3.12	0.67	4.08	0.44
f_A	peaks min^{-1}	124	17	37	5.1
F_0	cm^3 peak^{-1}	9.6	44.6	1.5	68.4
F	cm^3 peak^{-1}	0.24	1.80	0.16	5.85

$D_m = 1.5\times10^{-5}\,cm^2\,s^{-1}$, $\lambda/\nu = 0.07\,cm^{-2}\,s$.

that the minimum obtainable residence time due to the backpressure and the maximum flow depend more on the radius (squared power) than on the length.

The same analytical frequency can be achieved in straight tubes by reducing the tube radius. As an example, if the coil reactor increases in the analytical frequency fivefold, a straight tube of radius five times less would have the same analytical frequency. In turn, the carrier consumption can be drastically reduced; this is because F depends linearly on a^4. In the previous example, if a straight reactor is used, it will require a volume per peak of 625 times less.

This optimization only takes into account the transport contribution to dispersion. Nevertheless, it shows clearly, in a system optimization, how all the variables should be included and their influence on the different parameters that "make" the analytical performance.

Equation (36) shows a suitable way to select the variables of a system from which a certain analytical performance is required. It is worth mentioning that this equation is not a real optimization, as it minimizes the $\left(\frac{l}{L}\right)_{1/2}$ value as a function of the flow rate and/or the residence time. If this relation decreases, the absolute slope of the D vs. S_V curve increases, minimizing D and the peak width.

1.7 Concluding Remarks

In this chapter, we have presented a critical review of the different factors that are able to describe the dispersion process in flow systems. Mainly, the review was biased towards flow injection systems as these systems have been extensively studied from a theoretical point of view. Special emphasis was placed on the dispersion descriptors and on the relevance of finding global descriptors that allow the analyst to predict the best working conditions in order to maximize analytical frequency together with optimal sensitivity. Based on this, the relevance of knowing the influence of the different components of the flow system on the global dispersion was demonstrated by analyzing the different models reported to date. It was observed that, mainly, the different approaches pay no attention to the influence of detection and injection on global dispersion. Thus, it is important to stress that the different parts of a system can influence the obtained results, which obliges one to develop configurations where the contribution of the detector is negligible. Moreover, two different ways of selecting and optimizing a flow system in terms of the desired dispersion degree were shown.

It is clear that the analytical strength of the technique rests in controlling the diffusive processes of mixing, keeping the integrity of the injected sample plug. This needs to be attained through knowledge of the transport phenomena and the factors that influence them. In this way, the development of an equation able to relate global dispersion to the typical variables of FIA should be of great interest when predicting the behaviour of systems. However, the different theoretical models and experimental arrangements reported in the literature have failed in monitoring the mass redistribution and thus, dispersion, in a continuous way as time elapses.

Acknowledgments

The authors thank Dr. Osvaldo Troccoli for his contribution to this chapter.

References

1 Skeggs, L.J. (1957) An automatic method for colorimetric analysis. *American Journal of Clinical Pathology*, **28**, 311–322.

2 Ruzicka, J. and Hansen, E.H. (1975) Flow Injection Analysis. Part I. A new concept of fast continuous flow analysis. *Analytica Chimica Acta*, **78**, 145–157.

3 Ruzicka, J., Marshall, G.D. and Christian, G.D. (1990) Variable Flow Rates and Sinusoidal Flow Pump Flow Injection Analysis. *Analytical Chemistry*, **62**, 1861–1866.

4 Ruzicka, J. and Marshall, G.D. (1990) Sequential injection: a new concept for chemical sensors, process analysis and laboratory assays. *Analytica Chimica Acta*, **237**, 329–343.

5 Gubeli, T., Christian, G.D. and Ruzicka, J. (1991) Fundamentals of sinusoidal flow sequential injection spectrophotometry. *Analytical Chemistry*, **63**, 1861–1866.

6 Gubeli, T., Christian, G.D. and Ruzicka, J. (1991) Principles of stopped-flow sequential injection analysis and its application to the kinetic determination of traces of a proteolytic enzyme. *Analytical Chemistry*, **63**, 1680–1685.

7 Baron, A., Guzman, M., Ruzicka, J. and Christian, G.D. (1992) Novel single-standard calibration and dilution method performed by the sequential injection technique. *Analyst*, **117**, 1839–1844.

8 Masini, J.C., Baxter, P.J., Detwiler, K.R. and Christian, G.D. (1995) Online spectrophotometric determination of phosphate in bioprocesses by sequential injection. *Analyst*, **120**, 1583–1587.

9 van Staden, J.F. and Taljaard, R.E. (1997) Online dilution with sequential injection analysis: a system for monitoring sulfate in industrial effluents. *Fresenius' Journal of Analytical Chemistry*, **357**, 577–581.

10 Giné, M.F., Bergamin Filho, H. and Zagatto, E.A.G. (1980) Simultaneous determination of nitrate and nitrite by flow injection analysis. *Analytica Chimica Acta*, **114**, 191–197.

11 Krug, F.J., Bergamin Filho, H. and Zagatto, E.A.G. (1986) Commutation in flow injection analysis. *Analytica Chimica Acta*, **179**, 103–118.

12 Reis, B.F., Giné, M.F., Zagatto, E.A.G., Lima, J.L.F.C. and Lapa, R.A.S. (1994) Multicommutation in flow analysis. 1. Binary sampling: concepts, instrumentation and spectrophotometric determination of iron in plant digests. *Analytica Chimica Acta*, **293**, 129–138.

13 Reis, B.F., Morales-Rubio, A. and de la Guardia, M. (1999) Environmentally friendly analytical chemistry through automation: comparative study of strategies for carbaryl determination with p-aminophenol. *Analytica Chimica Acta*, **392**, 265–272.

14 Zagatto, E.A.G., Reis, B.F., Oliveira, C.C., Sartini, R.P. and Arruda, M.A.Z. (1999) Evolution of the commutation concept associated with the development of flow analysis. *Analytica Chimica Acta*, **400**, 249–256.

15 Christian, G.D. and Ruzicka, J. (1992) Exploiting stopped-flow injection methods for quantitative chemical analysis. *Analytica Chimica Acta*, **261**, 11–21.

16 Ruzicka, J. and Hansen, E.H. (1988) *Flow Injection Analysis*, Wiley, New York.

17 Honorato, R.S., Araujo, M.C.U., Lima, R.A.C., Zagatto, E.A.G., Lapa, R.A.S. and Costa Lima, J.L.F. (1999) A flow-batch titrator exploiting a one-dimensional

optimisation algorithm for end point search. *Analytica Chimica Acta*, **396**, 91–97.

18 Probstein, R.F. (1994) *Physicochemical Hydrodynamics: An Introduction*, John Wiley & Sons, New York.

19 Atkins, P.W. (1978) *Cap 26, 27 and Appendix Vol*, Addison-Wesley Iberoamericana, New York.

20 Brooks, S.H., Leff, D.V., Torres, M.H. and Dorsey, J.G. (1988) Dispersion coefficient and moment analysis of flow injection analysis peaks. *Analytical Chemistry*, **60**, 2737–2744.

21 Betteridge, D. and Ruzicka, J. (1976) Determination of glycerol in water by flow injection analysis – a novel way of measuring viscosity. *Talanta*, **23**, 409–410.

22 Pungor, E., Feher, Z., Nagy, G., Toth, K., Horvai, G. and Gratzl, M. (1979) Injection techniques in dynamic flow-through analysis with electrothermal analysis sensors. *Analytica Chimica Acta*, **109**, 1.

23 Streeter, V.L. and Wylie, E.G. (1981) *Mecánica de Fluídos*, McGraw-Hill, Bogot.

24 Taylor, G. (1953) Dispersion of soluble matter in solvent flowing through a tube. *Proceedings of the Royal Society of London, Series A*, **219**, 186–203.

25 Taylor, G. (1954) Conditions under which dispersion of a solute in a stream of solvent can be used to measure molecular difusion. *Proceedings of the Royal Society of London, Series A*, **225**, 473–477.

26 Levenspiel, O. (1962) *Chemical Reaction Engineering*, Wiley, New York.

27 Ruzicka, J. and Hansen, E.H. (1978) Flow injection analysis. Part X. Theory, Techniques and Trends. *Analytica Chimica Acta*, **99**, 37–76.

28 Painton, C.C. and Mottola, H.A. (1984) Kinetics in continuous flow sample processing. *Analytica Chimica Acta*, **158**, 67.

29 Painton, C.C. and Mottola, H.A. (1983) Dispersion in continuous-flow sample processing. *Analytica Chimica Acta*, **154**, 1–16.

30 Ananthakrishnan, V., Gill, W.N. and Barduhn, A.J. (1965) Laminar dispersion in capillaries. 1. Mathematical analysis. *American Institute of Chemical Engineers Journal*, **11**, 1063.

31 Li, Y.S. and Gao, X.F. (1996) Two new parameters: Axial dispersion degree and radial dispersion intensity of sample zone injected in flow injection analysis systems. *Laboratory Robotics and Automation*, **8**, 351.

32 Johnson, B.F., Malick, R.E. and Dorsey, J.G. (1992) Reduction of injection variance in flow injection analyisis. *Talanta*, **39**, 35–44.

33 Brooks, S.H. and Rullo, G. (1990) Minimal dispersion flow injection analysis systems for automated sample introduction. *Analytical Chemistry*, **62**, 2059–2062.

34 Spence, D.M. and Crouch, S.R. (1997) Factors affecting zone variance in a capillary flow injection system. *Analytical Chemistry*, **69**, 165–169.

35 Levenspiel, O., Lai, B.W. and Chatlynne, C.Y. (1970) Tracer curves and residence time distribution. *Chemical Engineering Science*, **25**, 1611–1613.

36 Levenspiel, O. and Turner, J.C.R. (1970) The interpretation of residence-time experiments. *Chemical Engineering Science*, **25**, 1605–1609.

37 Snyder, L.R. (1980) Continuous-flow analysis: present and future. *Analytica Chimica Acta*, **114**, 3–18.

38 Foley, J.P. and Dorsey, J.G. (1983) Equations for calculation of chromatographic figures of merit for ideal and skewed peaks. *Analytical Chemistry*, **55**, 730–737.

39 Betteridge, D., Cheng, W.C., Dagless, E.L., David, P., Goad, T.B., Deans, D.R., Newton, D.A. and Pierce, T.B. (1983) An automated viscometer based on high-precision flow injection analysis. 2. Measurement of viscosity and diffusion-coefficients. *Analyst*, **108**, 17.

40 Stone, D.C. and Tyson, J.F. (1986) Flow cell and diffusion-coefficient effects in flow injection analysis. *Analytica Chimica Acta*, **179**, 427.

41 van Staden, J.F. (1990) Effect of coated open-tubular inorganic-based solid-state ion-selective electrodes on dispersion in flow injection. *Analyst*, **115**, 581–585.

42 van Staden, J.F. (1992) Response-time phenomena of coated open-tubular solid-state silver-halide selective electrodes and their influence on sample dispersion in flow injection analysis. *Analytica Chimica Acta*, **261**, 381.

43 Vanderslice, J.T., Rosenfeld, A.G. and Beecher, G.R. (1986) Laminar-flow bolus shapes in flow injection analysis. *Analytica Chimica Acta*, **179**, 119–129.

44 Ruzicka, J., Hansen, E.H. and Zagatto, E.A. (1977) Flow injection analysis. 7. Use of ion-selective electrodes for rapid analysis of soil extracts and blood serum. Determination of potassium, sodium and nitrate. *Analytica Chimica Acta*, **88**, 1–16.

45 Korenaga, T. (1992) Aspects of sample dispersion for optimizing flow injection analysis systems. *Analytica Chimica Acta*, **261**, 539.

46 Narusawa, Y. and Miyamae, Y. (1994) Zone circulating flow injection analysis: theory. *Analytica Chimica Acta*, **289**, 355–364.

47 Narusawa, Y. and Miyamae, Y. (1994) Radial dispersion by computer-aided simulation with data from zone circulating flow injection analysis. *Analytica Chimica Acta*, **296**, 129–140.

48 Narusawa, Y. and Miyamae, Y. (1995) Evidence of axial diffusion accompanied by axial dispersion with zone circulating flow injection analysis data. *Analytica Chimica Acta*, **309**, 227–239.

49 Narusawa, Y. and Miyamae, Y. (1998) Decisive problems of zone-circulating flow injection analysis and its solution. *Talanta*, **45**, 519.

50 Vanderslice, J.T., Stewart, K.K., Rosenfeld, A.G. and Higgs, D.H. (1981) Laminar dispersion in flow injection analysis. *Talanta*, **28**, 11–18.

51 Vanderslice, J.T., Beecher, G.R. and Rosenfeld, A.G. (1984) Dispersion and diffusion coefficients in flow injection analysis. *Analytica Chimica Acta*, **56**, 292–293.

52 Gomez-Nieto, M.A., Luque de Castro, M.D., Martin, A. and Valcarcel, M. (1985) Prediction of the behavior of a single flow injection manifold. *Talanta*, **32**, 319–324.

53 Kempster, P.L., van Vliet, H.R. and Staden, J.F. (1989) Prediction of FIA peak width for a flow injection manifold with spectrophotometric or ICP detection. *Talanta*, **36**, 969.

54 Tijssen, R. (1980) Axial dispersion and flow phenomena in helically coiled tubular reactors for flow analysis and chromatography. *Analytica Chimica Acta*, **114**, 71–89.

55 Reijn, J.M., van der Linden, W.E. and Poppe, H. (1981) Transport phenomena in flow injection analysis without chemical reaction. *Analytica Chimica Acta*, **126**, 1.

56 Andrade, F.J., Iñón, F.A., Tudino, M.B. and Troccoli, O.E. (1999) Integrated conductimetric detection: mass distribution in a dynamic sample zone inside a flow injection manifold. *Analytica Chimica Acta*, **379**, 99–106.

57 Iñón, F.A., Andrade, F.J. and Tudino, M.B. (2003) Mass distribution in a dynamic sample zone inside a flow injection manifold: modelling integrated conductimetric profiles. *Analytica Chimica Acta*, **477**, 59–71.

58 Golay, M.J.E. and Atwood, J.G. (1979) Early phases of the dispersion of a sample injected in poiseuille flow. *Journal of Chromatography*, **186**, 353–370.

59 Atwood, J.G. and Golay, M.J.E. (1981) Dispersion of peaks by short straight open tubes in liquid-chromatography systems. *Journal of Chromatography*, **218**, 97–122.

60 Poppe, H. (1980) Characterization and design of liquid phase flow-through detector system. *Analytica Chimica Acta*, **114**, 59–70.

61 Reijn, J.M., van der Linden, W.E. and Poppe, H. (1980) Some theroretical aspects of flow injection analysis. *Analytica Chimica Acta*, **114**, 105–118.

62 Valcárcel, M. and Luque de Castro, M.D. (1987) *Flow injection analysis: Principles and Applications*, Ellis Horwood, Chichester.

63 Coq, B., Cretier, G., Rocca, J.L. and Porthault, M. (1981) Open or packed sampling loops in liquid-chromatography. *Journal of Chromatographic Science*, **19**, 12–112.

64 Kolev, S.D. (1995) Mathematical modelling of flow inject systems. *Analytica Chimica Acta*, **308**, 36–66.

65 DeLon Hull, R., Malic, R.E. and Dorsey, J.G. (1992) Dispersion phenomena in flow injection systems. *Analytica Chimica Acta*, **267**, 1–24.

66 Brooks, S.H. and Dorsey, J.G. (1990) Moment analysis for evaluation of flow injection manifolds. *Analytica Chimica Acta*, **229**, 35.

67 Ramsing, A.U., Ruzicka, J. and Hansen, E.H. (1981) The principles and theory of high-speed titrations by flow injection analysis. *Analytica Chimica Acta*, **129**, 1.

68 Reijn, J.M., Poppe, H. and van der Linden, W.E. (1984) Kinetics in a single bead string reactor for flow injection analysis. *Analytical Chemistry*, **56**, 943–948.

69 Hartnett, M., Diamond, D. and Barker, P.G. (1993) Neural network-based recognition of flow injection patterns. *Analyst*, **118**, 347–354.

70 Hungerford, J.M. and Christian, G.D. (1987) Chemical kinetics with reagent dispersion in single-line flow injection systems. *Analytica Chimica Acta*, **200**, 1.

71 Tyson, J.F. and Idris, A.B. (1981) Flow injection sample introduction for atomic absorption spectrometry: Applications of a simplified model for dispersion. *Analyst*, **106**, 1125.

72 Burguera, J.L. (1989) *Flow Injection Atomic Spectroscopy*, Marcel Dekker, New York.

73 Betteridge, D., Marczewski, C.Z. and Wade, A.P. (1984) A random walk simulation of flow injection analysis. *Analytica Chimica Acta*, **165**, 227–236.

74 Crowe, C.D., Levin, H.W., Betteridge, D. and Wade, A.P. (1987) A random-walk simulation of flow injection sytems with merging zones. *Analytica Chimica Acta*, **194**, 49.

75 Wentzell, P.D., Bowdridge, M.R., Taylor, E.L. and Macdonald, C. (1993) Random-walk simulation of flow injection analysis — evaluation of dispersion profiles. *Analytica Chimica Acta*, **278**, 293–306.

76 Levine, I.N.(1988) *Chapter 16*, McGraw-Hill, Madrid.

77 Iñón, F.A. (2001) in Un nuevo enfoque en el estudio del proceso de dispersión en FIA: el método conductimétro integral (ICM) y modelado matemático de las curvas ICM Vol. Ph. D. Universidad de Buenos Aires, Buenos Aires, p. 464.

78 Reijn, J.M., Poppe, H. and van der Linden, W.E. (1983) A possible approach to the optimization of flow injection analysis. *Analytica Chimica Acta*, **145**, 59.

79 Betteridge, D. (1978) Flow injection analysis. *Analytical Chemistry*, **50**, 832A–846.

80 Andrade, F.J. (2001) in Estudio de dispersión en sistemas de análisis por inyección en flujos (FIA) y su aplicación al análisis de vestigios Vol. Ph. D. Universidad de Buenos Aires, Buenos Aires, p. 381.

81 Leclerc, D.F., Bloxham, P.A. and Toren, E.C.J. (1986) Axial dispersion in coiled tubular reactors. *Analytica Chimica Acta*, **184**, 173.

82 Li, Y.H. and Ma, H.C. (1995) Two trends of sample dispersion variation with carrier flow rate in a single flow injection manifold. *Talanta*, **42**, 2033.

83 Stone, D.C. and Tyson, J.F. (1987) Models for dispersion in flow injection analysis. 1. basic requirements and study of factors affecting dispersion. *Analyst*, **112**, 515–521.

84 Fang, Z. (1995) *Flow Injection Atomic Absorption Spectrometry*, John Wiley & Son Ltd, New York.

85 Reijn, J.M., van der Linden, W.E. and Poppe, H. (1980) Dispersion phenomena in reactors for flow analysis. *Analytica Chimica Acta*, **114**, 91–104.